Supporting Information

Manipulating Metal-Ligand Binding in Allosteric Coordination Complexes through Ring Strain

Yiming Hu,[†‡] Fiona Yihan Wang,[†‡] Yi Xie,[†] Benjamin D. Coleman,[†] Charlotte L. Stern,[†] and Chad A. Mirkin[†*]

[*]Corresponding author

[†]Department of Chemistry and International Institute for Nanotechnology, Northwestern University, Evanston, Illinois 60208, United States

Contact email: chadnano@northwestern.edu

Table of Contents

Materials and Methods

All syntheses were performed under N_2 atmosphere using standard Schlenk techniques. All chemicals, reagents, and solvents were purchased as reagent grade from Sigma Aldrich, TCI, and Alfa Aesar and were used without further purification. Solvents were dried over activated 3 Å molecular sieves for 48 hours prior to use. All glassware and stir bars were flamed-dried prior to use. Flash chromatography was performed using SiO_2 60 (230–400 mesh ASTM, 0.040–0.063 mm; Fluka). Deuterated solvents were purchased from Cambridge Isotope Laboratories and used as received. ^{1}H, ^{13}C, $^{31}P\{^{1}H\}$, and ^{195}Pt NMR spectra were recorded on a Bruker Avance HD 500 MHz and Bruker Avance III 600 MHz NMR spectrometers. ^{1}H NMR spectra were referenced to residual proton resonances in the corresponding deuterated solvents, while absolute referencing was applied for heteronuclear NMR spectra. High resolution mass spectra (HR-MS) were recorded on an Agilent 6120 LC-TOF instrument in positive ion mode. Suitable single crystals were selected and mounted on a MITIGEN holder in Paratone oil on a Bruker Kappa APEX-II CCD diffractometer. All measurements were made with graphite-monochromated Mo Kα radiation. Using Olex2, the structure was solved with the SHELXT structure solution program, using Intrinsic Phasing and refined with the SHELXL refinement package using Least Squares minimization.

Synthesis

General procedure for ligand synthesis

[(Chloromethyl)thio]benzene and [(2-Chloroethyl)thio]benzene were purchased directly without further purification. [(3-Chloropropyl)thio]benzene, [(4-Chlorobutyl)thio]benzene, and [(5-Chloropentyl)thio]benzene were prepared by following the literature procedure.[1]

Ligands **7a-e** were prepared based on a modification of a reported procedure.[2] To a solution of diphenylphosphine (186 mg, 1 mmol) in anhydrous THF (10 mL) was added 2.5M *n*BuLi (0.40 mL, 1 mmol) at -78 °C. The reaction was left to stir for 1h while warming up to room temperature to afford an orange solution. (1 mmol) dissolved in anhydrous THF (10 mL) was added dropwise to the orange solution. The reaction was left to stir at -78 °C overnight and quenched with MeOH (1 mL). Upon vacuum filtration, the reaction was concentrated *in vacuo* and purified via flash column chromatography on silica gel (hexanes:DCM = 7:3). The product fraction was dried *in vacuo* to obtain a white solid (80-95% yield). ^{1}H NMR spectra of **7a-c** agreed with literature spectra.[3-5]

General procedure for complex synthesis

The complex precursor **8** was prepared according to reported procedures.[6]

The complexes **5a**, **4b**, **4c**, **5d**, **5e** were synthesized using procedures adapted from the literature method.[7] Under N_2 atmosphere, **8** (30 mg, 0.068 mmol) and $AgBF_4$ (29.1 mg, 0.15 mmol) were suspended in a mixture of anhydrous acetonitrile (2 mL) and dichloromethane (2 mL). The suspension was stirred in the dark at room temperature for 1 hour. Then, the mixture was filtered using a PTFE syringe filter (pore size 0.45 µm), and the filtrate was added to a solution of ligand **7a-e** (0.068 mmol) in anhydrous dichloromethane (2 mL). The resulting solution was stirred for 1 hour and concentrated *in vacuo*. The crude product was washed with hexanes (5 mL) and diethylether (5 mL) thrice to afford a white solid. The product was further purified by recrystallization.

7d. ^{1}H NMR (500 MHz, $CDCl_3$) δ 7.45 (m, 4H), 7.36 – 7.33 (m, 10H), 7.21 – 7.18 (m, 1H), 2.93 (t, J = 7.4 Hz, 2H), 2.09 (t, J = 8.0 Hz, 2H), 1.81 (tt, J = 7.5, 7.4 Hz, 2H), 1.62 (m, 2H). ^{13}C NMR (126 MHz,

$CDCl_3$) δ 138.79, 138.69, 136.74, 132.86, 132.71, 129.24, 128.92, 128.64, 128.53, 128.48, 125.90, 33.34, 30.60 (d, $J_{C\text{-}C}$ = 12.9 Hz), 27.71 (d, $J_{C\text{-}C}$ = 11.8 Hz), 25.24 (d, $J_{C\text{-}P}$ = 16.5 Hz).

7e. ^{1}H NMR (500 MHz, $CDCl_3$) δ 7.37 (m, 7H), 7.26 – 7.21 (m, 7H), 7.12 (m, 1H), 2.84 (t, *J* = 7.2 Hz, 2H), 2.00 (t, *J* = 7.9 Hz, 2H), 1.60 (tt, *J* = 7.3, 7.2 Hz, 2H), 1.53 (tt, *J* = 7.9, 7.5 Hz, 2H), 1.42 (m, 2H). ^{13}C NMR (126 MHz, $CDCl_3$) δ 138.87, 138.77, 136.96, 132.91, 132.76, 129.13, 128.97, 128.82, 128.68, 128.57, 128.54, 128.51, 125.87, 33.57, 30.39 (d, $J_{C\text{-}C}$ = 13.0 Hz), 28.88, 28.00 (d, $J_{C\text{-}C}$ = 11.0 Hz), 25.62 (d, $J_{C\text{-}P}$ = 16.2 Hz).

5a. ^{1}H NMR (500 MHz, CD_3CN) δ 7.86 (dd, *J* = 6.0, 3.5 Hz, 2H), 7.60 (m, 6H), 7.48 (m, 3H), 7.36 (m, 3H), 7.31 – 7.23 (m, 4H), 6.83 (m, 1H), 6.28 (d, *J* = 6.8 Hz, 1H), 6.10 (d, *J* = 6.8 Hz, 1H), 4.29 (dd, *J* = 14.0, 7.8 Hz, 1H), 4.07 (dd, *J* = 14.0, 6.7 Hz, 1H), 3.80 (s, 3H), 3.05 (s, 3H). ^{31}P{^{1}H} NMR (243 MHz, CD_3CN) δ 6.88 ($J_{Pt\text{-}P}$ = 2445 Hz). ^{195}Pt NMR (128 MHz, CD_3CN) δ -4328.88 (d, $J_{Pt\text{-}P}$ = 2461 Hz). HRMS (ESI^{+}) m/z Cal'd for $[C_{30}H_{36}N_5PPtS]^{+}$: 724.2077. Found: 724.1511. Single crystals suitable for X-ray diffraction studies were obtained by slow diffusion of methyl *t*-butyl ether into a MeCN solution of **5a**.

6a. ^{1}H NMR (600 MHz, CD_3CN) δ 8.00 (dd, *J* = 10.9, 7.8 Hz, 2H), 7.63 (m, 3H), 7.55 (m, 4H), 7.42 (m, 1H), 7.32 – 7.24 (m, 8H), 6.71 (m, 2H), 6.27 (d, *J* = 13.1 Hz, 1H), 4.37 (dd, *J* = 13.1, 6.8 Hz, 1H), 4.10 (dd, *J* = 13.1, 8.6 Hz, 1H), 3.93 (s, 3H), 2.92 (s, 3H). ^{31}P{^{1}H} NMR (243 MHz, CD_3CN) δ 9.81 ($J_{Pt\text{-}P}$ = 2528 Hz). ^{195}Pt NMR (128 MHz, CD_3CN) δ -4191.91 (d, $J_{Pt\text{-}P}$ = 2528 Hz). HRMS (ESI^{+}) m/z Cal'd for $[C_{28}H_{32}ON_4PPtS]^{+}$: 698.1682. Found: 698.1521.

4b. ^{1}H NMR (500 MHz, CD_3CN) δ 7.89 (dd, 2H), 7.69 (m, 8H), 7.55 (m, 7H), 6.99 (m, 1H), 6.93 (d, *J* = 1.2 Hz, 1H), 6.09 (m, 2H), 3.77 (s, 3H), 3.25 (m, 1H), 3.07 (m, 1H), 3.05 (s, 3H), 3.01 (m, 1H), 2.85 (m, 1H). ^{31}P{^{1}H} NMR (243 MHz, CD_3CN) δ 42.54 ($J_{Pt\text{-}P}$ = 2402 Hz). ^{195}Pt NMR (128 MHz, CD_3CN) δ -4673.61 (d, $J_{Pt\text{-}P}$ = 2412 Hz). Single crystals suitable for X-ray diffraction studies were obtained by slow diffusion of methyl *t*-butyl ether into a MeCN solution of **4b**.

6b. ^{1}H NMR (600 MHz, CD_3CN) δ 7.91 (dd, *J* = 5.6, 3.5 Hz, 2H), 7.61 (m, 1H), 7.55 (m, 4H), 7.30 (m, 6H), 7.25 (m, 2H), 7.14 (m, 1H), 6.70 (m, 1H), 6.33 (m, 2H), 3.67 (s, 3H), 3.51 (m, 1H), 3.31 (m, 1H), 2.98 (m, 1H), 2.84 (s, 3H), 2.79 (m, 1H). ^{31}P{^{1}H} NMR (243 MHz, CD_3CN) δ 9.08 ($J_{Pt\text{-}P}$ = 2483 Hz). ^{195}Pt NMR (128 MHz, CD_3CN) δ -4199.61 (d, $J_{Pt\text{-}P}$ = 2489 Hz). HRMS (ESI^{+}) m/z Cal'd for $[C_{29}H_{34}ON_4PPtS]^{+}$: 712.1839, Found: 712.1609. Single crystals suitable for X-ray diffraction studies were obtained by slow diffusion of methyl *t*-butyl ether into a MeCN solution of **6b**.

4c. ^{1}H NMR (500 MHz, CD_3CN) δ 8.32 (dd, J = 11.9, 7.0 Hz, 2H), 7.85 (m, 3H), 7.61 (d, J = 7.4 Hz, 2H), 7.40 (m, 10H), 6.67 (d, J = 4.1 Hz, 2H), 6.53 (d, J = 2.0 Hz, 1H), 6.09 (d, J = 13.6 Hz, 1H), 3.52 (td, J = 11.1, 1.6 Hz, 1H), 3.39 (m, 1H), 3.18 (s, 3H), 2.96 (m, 4H), 2.63 (m, 2H), 1.70 (m, 1H). ^{31}P{^{1}H} NMR (243 MHz, CD_3CN) δ -6.73 ($J_{Pt\text{-}P}$ = 2335 Hz). ^{195}Pt NMR (128 MHz, CD_3CN) δ -4490.82 (d, $J_{Pt\text{-}P}$ = 2341 Hz). Single crystals suitable for X-ray diffraction studies were obtained by slow diffusion of methyl *t*-butyl ether into a MeCN solution of 4c**.**

6c. ^{1}H NMR (600 MHz, CD_3CN) δ 8.35 (dd, J = 5.9, 3.6 Hz, 1H), 7.82 (m, 3H), 7.60 (m, 2H), 7.48 (m, 3H), 7.25 (m, 14H), 6.61 (m, 2H), 6.06 (dd, J = 10.0, 6.8 Hz, 1H), 5.90 (d, J = 13.4 Hz, 1H), 3.92 (s, 3H), 3.03 (m, 1H), 2.81 (m, 4H), 2.65 (m, 2H), 2.25 (m, 1H), 2.02 (m, 1H). ^{31}P{^{1}H} NMR (243 MHz, CD_3CN) δ 10.21 ($J_{Pt\text{-}P}$ = 2500 Hz). ^{195}Pt NMR (128 MHz, CD_3CN) δ -4200.79 (d, $J_{Pt\text{-}P}$ = 2484 Hz). HRMS (ESI^{+}) m/z Cal'd for $[C_{30}H_{36}ON_4PPtS]$+: 726.1995, Found: 726.2364.

4d. ^{1}H NMR (600 MHz, CD_2Cl_2) δ 8.24 (m, 2H), 7.88 (m, 3H), 7.47 (m, 10H), 7.30 (m, 2H), 7.10 (m, 2H), 6.80 (d, J = 13.6 Hz, 1H), 6.61 (m, 1H), 6.48 (d, J = 1.8 Hz, 1H), 6.26 (d, J = 13.8 Hz, 1H), 3.50 (s, 3H), 3.00 (m, 1H), 2.94 (s, 3H), 2.82 (m, 1H), 2.66 (m, 2H), 2.27 (m, 1H), 1.74 (m, 1H), 1.56 (m, 2H). ^{31}P{^{1}H} NMR (243 MHz, CD_2Cl_2) δ 17.03 ($J_{Pt\text{-}P}$ = 2466 Hz). ^{195}Pt NMR (128 MHz, CD_2Cl_2) δ -4467.43 (d, $J_{Pt\text{-}P}$ = 2524 Hz). Single crystals suitable for X-ray diffraction studies were obtained by slow diffusion of methyl *t*-butyl ether into a CH_2Cl_2 solution of **4d**.

5d. . ^{1}H NMR (600 MHz, CD_3CN) δ 7.70 (m, 2H), 7.57 (m, 9H), 7.41 (m, 1H), 7.29 (m, 4H), 7.20 (m, 2H), 6.86 (d, J = 2.0 Hz, 1H), 6.30 (d, J = 13.5 Hz, 1H), 6.10 (d, J = 13.6 Hz, 1H), 3.84 (s, 3H), 3.04 (s, 3H), 2.95 (m, 2H), 2.64 (m, 1H), 2.49 (m, 1H), 1.85 (m, 1H), 1.70 (m, 3H). ^{31}P{^{1}H} NMR (243 MHz, CD_2Cl_2) δ 7.55 ($J_{Pt\text{-}P}$ = 2381 Hz). ^{31}P{^{1}H} NMR (243 MHz, CD_3CN) δ 7.64 ($J_{Pt\text{-}P}$ = 2394 Hz). ^{195}Pt NMR (128 MHz, CD_2Cl_2) δ -4341.34 (d, $J_{Pt\text{-}P}$ = 2387 Hz). ^{195}Pt NMR (128 MHz, CD_3CN) δ -4340.78 (d, $J_{Pt\text{-}P}$ = 2408 Hz). Single crystals suitable for X-ray diffraction studies were obtained by slow diffusion of methyl *t*-butyl ether into a MeCN solution of **5d**.

6d. ^{1}H NMR (600 MHz, CD_3CN) δ 7.87 (dd, J = 4.2, 3.8 Hz, 2H), 7.62 (m, 1H), 7.54 (m, 2H), 7.44 (m, 4H), 7.32 (m, 7H), 7.21 (m, 1H), 7.16 (m, 1H), 6.73 (d, J = 1.9 Hz, 1H), 6.32 (d, J = 13.3 Hz, 1H), 6.02 (d, J = 13.4 Hz, 1H), 3.99 (s, 3H), 2.99 (m, 2H), 2.89 (s, 3H), 2.74 (m, 1H), 2.52 (m, 1H), 2.06 (m, 1H), 1.90 (m, 1H), 1.79 (m, 2H). ^{31}P{^{1}H} NMR (243 MHz, CD_2Cl_2) δ 10.58 ($J_{Pt\text{-}P}$ = 2488 Hz). ^{31}P{^{1}H} NMR (243 MHz, CD_3CN) δ 10.30 ($J_{Pt\text{-}P}$ = 2503 Hz). ^{195}Pt NMR (128 MHz, CD_2Cl_2) δ -4197.43 (d, $J_{Pt\text{-}P}$ = 2218 Hz). ^{195}Pt NMR (128 MHz, CD_3CN) δ -4198.80 (d, $J_{Pt\text{-}P}$ = 2482 Hz).

5e. ^{1}H NMR (500 MHz, CD_3CN) δ 7.73 (m, 2H), 7.51 (m, 15H), 7.33 (m, 3H), 7.23 (m, 2H), 6.87 (d, J = 2.0 Hz, 1H), 6.33 (d, J = 13.5 Hz, 1H), 6.10 (d, J = 13.6 Hz, 1H), 3.86 (s, 3H), 3.07 (s, 3H), 2.94 (m, 2H), 2.66 (m, 1H), 2.52 (m, 1H), 1.74 (m, 1H), 1.60 (m, 5H). ^{31}P{^{1}H} NMR (243 MHz, CD_3CN) δ 7.51 ($J_{Pt\text{-}P}$ = 2394 Hz). ^{195}Pt NMR (128 MHz, CD_3CN) δ -4340.96 (d, $J_{Pt\text{-}P}$ = 2413 Hz). Single crystals suitable for X-ray diffraction studies were obtained by slow diffusion of methyl *t*-butyl ether into a MeCN solution of **5e**.

6e. ^{1}H NMR (600 MHz, CD_3CN) δ 8.03 (d, J = 1.9 Hz, 1H), 7.87 (m, 3H), 7.60 (m, 3H), 7.44 (d, J = 12.9 Hz, 2H), 7.25 (m, 8H), 7.10 (m, 1H), 6.96 (m, 1H), 6.55 (d, J = 2.0 Hz, 1H), 6.07 (d, J = 12.8 Hz, 1H), 3.97 (s, 3H), 2.86 (dd, J = 7.1, 7.0 Hz, 2H), 2.83 (s, 3H), 2.66 (m, 1H), 2.42 (m, 1H), 1.91 (m, 1H), 1.70 (m, 1H), 1.50 (m, 3H), 1.26 (m, 1H). ^{31}P{^{1}H} NMR (243 MHz, CD_3CN) δ 10.19 ($J_{Pt\text{-}P}$ = 2503 Hz). ^{195}Pt NMR (128 MHz, CD_3CN) δ -4190.88 (d, $J_{Pt\text{-}P}$ = 2490 Hz). HRMS (ESI^{+}) m/z Cal'd for $[C_{32}H_{40}ON_4PPtS]$+: 754.2308, Found: 754.2097.

Dynamic Ligand Displacement Reactions

General procedure for ligand displacement reactions for 5a, 4b, 4c, 5d, 5e

A CD_3CN (2 mL) solution of recrystallized complexes (0.05 mmol) was charged with tetrabutylammonium chloride (2 equiv.) and stirred for 1 hour at room temperature.

Subsequently, the solution was charged with silver tetrafluoroborate (2 equiv.) and stirred for 1 hour at room temperature in dark. The suspension was filtered using a PTFE syringe filter (pore size 0.45 µm).

$^{31}P\{^1H\}$ and ^{195}Pt NMR spectra in CD_3CN were taken directly without further purification to characterize the respective structural states as shown below.

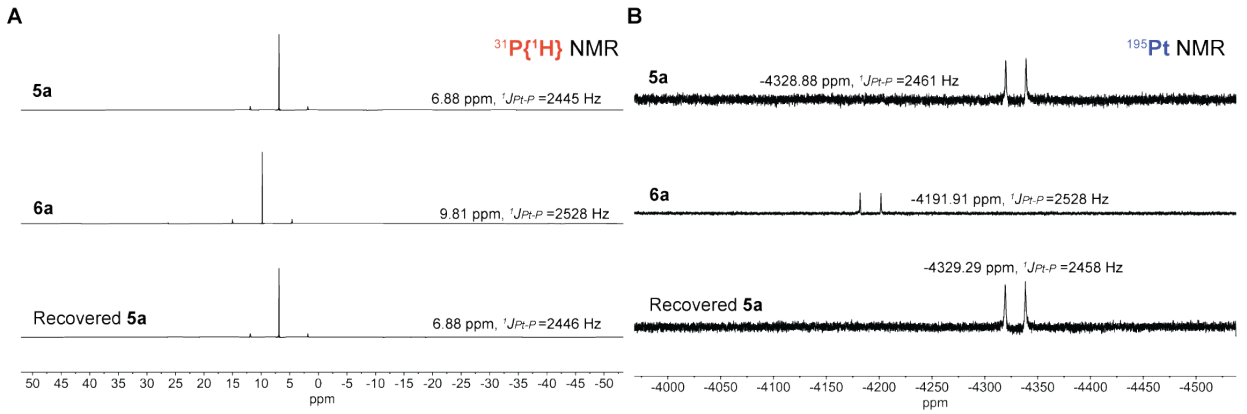

Figure S1. A. $^{31}P\{^1H\}$ and B. ^{195}Pt NMR spectra of **5a** and **6a** in dynamic ligand displacement reaction.

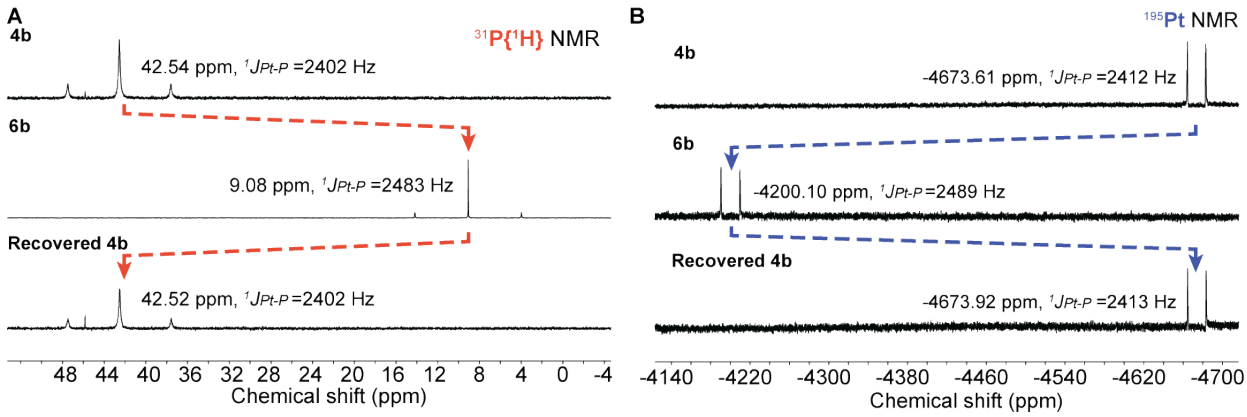

Figure S2. A. $^{31}P\{^1H\}$ and B. ^{195}Pt NMR spectra of **4b** and **6b** in the dynamic ligand displacement reaction.

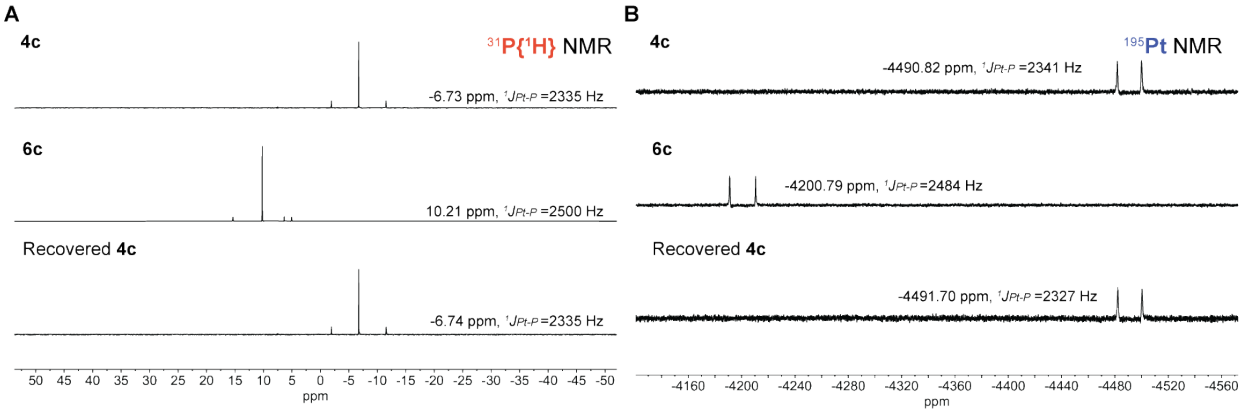

Figure S3. A. $^{31}P\{^{1}H\}$ and B. ^{195}Pt NMR spectra of **4c** and **6c** in the dynamic ligand displacement reaction.

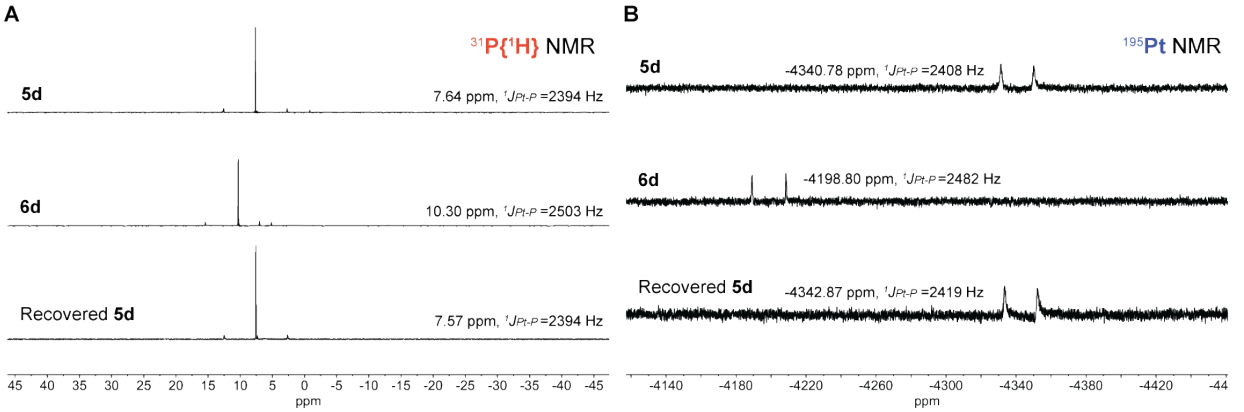

Figure S4. A. $^{31}P\{^{1}H\}$ and B. ^{195}Pt NMR spectra of **5d** and **6d** in the dynamic ligand displacement reaction.

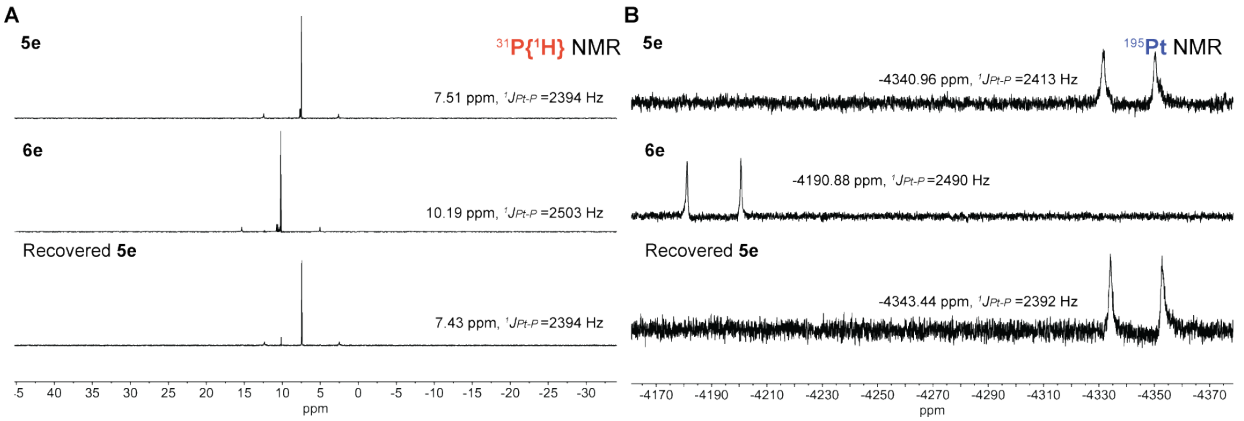

Figure S5. A. $^{31}P\{^{1}H\}$ and B. ^{195}Pt NMR spectra of **5e** and **6e** in the dynamic ligand displacement reaction.

General procedure for closing 5a, 5d, 5e complexes and their corresponding ligand displacement experiments

To obtain the closed complexes, recrystallized **5a**, **5d**, **5e** complexes (0.05 mmol) were dried *in vacuo* for 18 hours. The obtained products were then subjected to ligand displacement experiments as detailed below.

A deuterated dichloromethane (2 mL) solution of the obtained **5a**, **5d**, **5e** complexes (0.05 mmol) was charged with acetonitrile (10 equiv.) and stirred for 1 hour at room temperature.

Subsequently, the above solution was charged with tetrabutylammonium chloride (2 equiv.) and stirred for 1 hour at room temperature.

Lastly, silver tetrafluoroborate (2 equiv.) was added and stirred for 1 hour in the dark. The mixture was filtered using a PTFE syringe filter (pore size 0.45µm).

$^{31}P\{^{1}H\}$ and ^{195}Pt NMR spectra were taken directly without further purification to characterize the respective structural states as shown below.

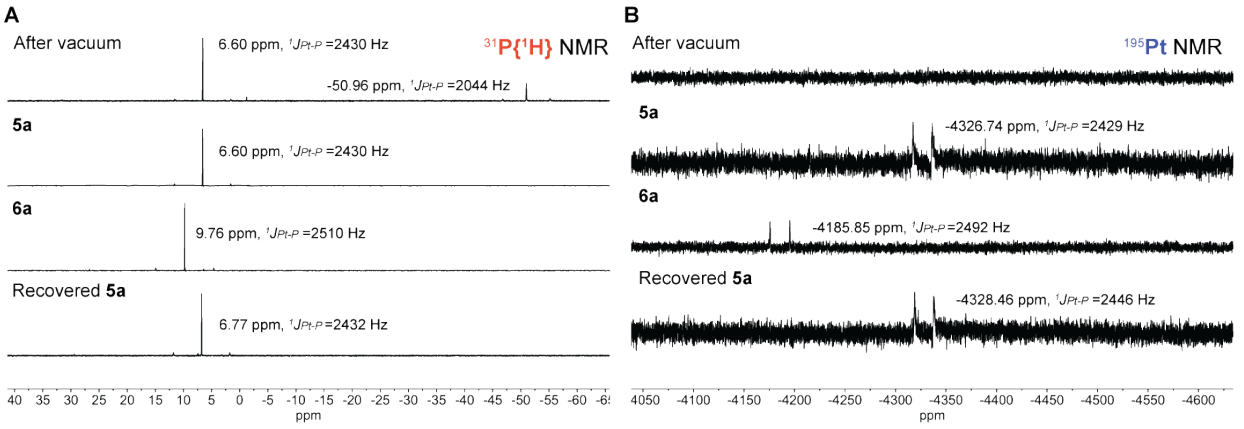

Figure S6. A. $^{31}P\{^{1}H\}$ and B. ^{195}Pt NMR spectra of **5a** after vacuum, **5a** and **6a** in the dynamic ligand displacement reaction. After drying *in vacuo* for 18 hours, **5a** showed limited solubility in dichloromethane which resulted in low signal intensity in the ^{195}Pt NMR spectrum.

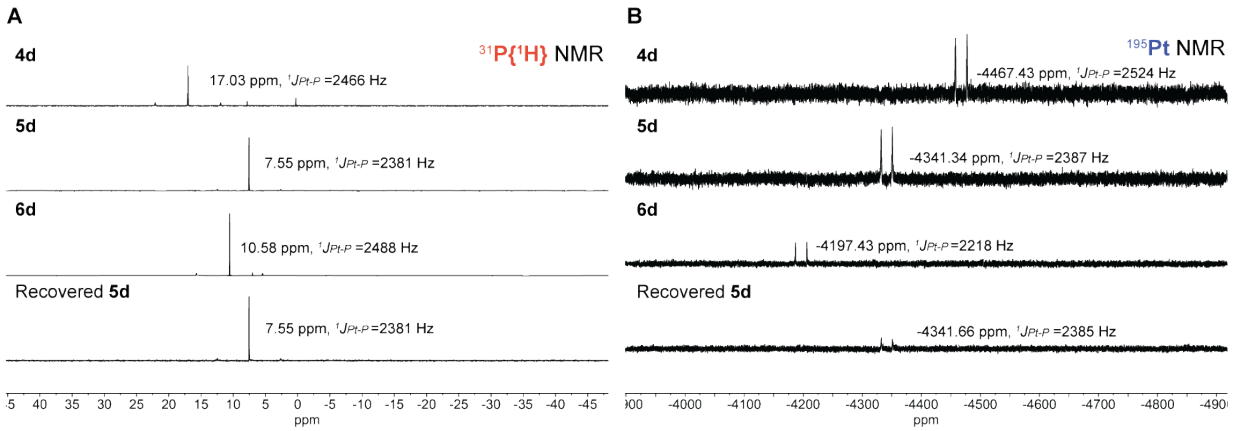

Figure S7. A. $^{31}P\{^{1}H\}$ and B. ^{195}Pt NMR spectra of **4d**, **5d**, and **6d** in the dynamic ligand displacement reaction.

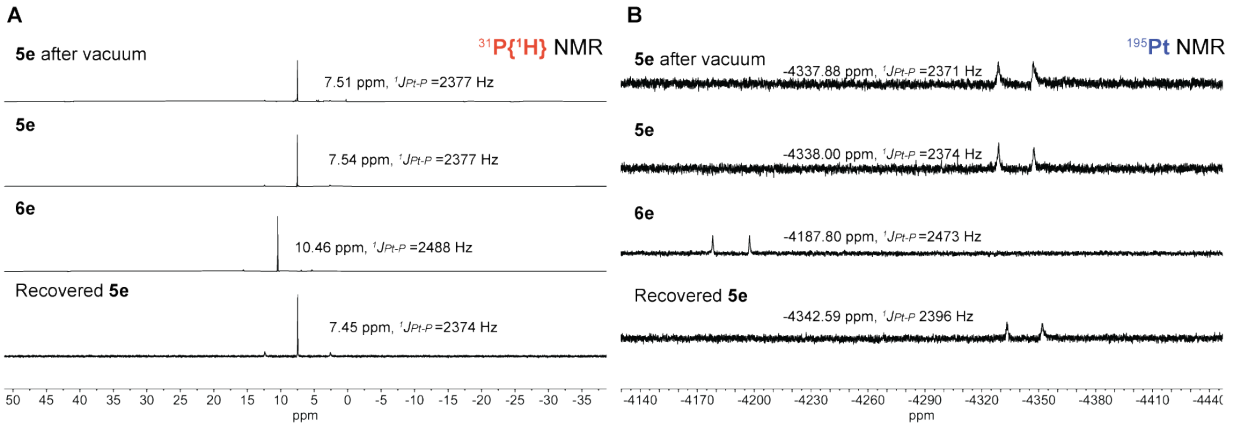

Figure S8. A. $^{31}P\{^{1}H\}$ and B. ^{195}Pt NMR spectra of **5e** after vacuum, **5e**, and **6e** in the dynamic ligand displacement reaction.

Solvent Effect Study

To ensure that changes in chemical shifts in $^{31}P\{^{1}H\}$ and ^{195}Pt NMR spectra are not affected changes in the solvent environment, **5d** and **6d** were dissolved in deuterated CD_3CN and CD_2Cl_2 respectively.

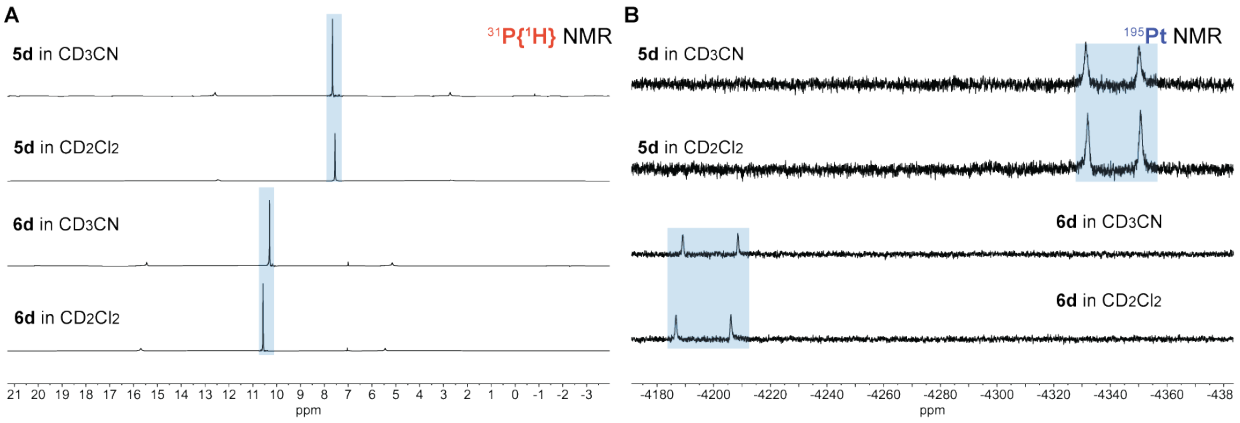

Figure S9. A. $^{31}P\{^{1}H\}$ and B. ^{195}Pt NMR spectra of **5d** and **6d** in CD_3CN and CD_2Cl_2 show that solvent has minimal effect on NMR chemical shifts and coupling constants.

Computational Studies

Dispersion-corrected DFT calculations (DFT-D) were performed using density functional theory (DFT) in the Dmol^3 code.[8] The generalized gradient approximation (GGA) with the Perdew-Burke-Ernzerhof (PBE) functional[9] and double Nnumerical plus polarization, with addition of diffuse functions (DNP+) basis set as well as the DFT semi-core pseudopotentials (DSPP) were used, with Tkatchenko-Scheffler (TS) semi-empirical methods employed to describe the long-range van der Waals interactions.[10] The energy, gradient and displacement convergence criteria were set as 1×10^{-5} Ha, 2×10^{-3} Å and 5×10^{-3} Å, respectively. The Pt-NHC complex structure model is adapted based on single crystal structure data, while the simplified *cis*-$PtCl_2$ complex models are built to provide reliable ring strain energy by reducing computational cost and avoiding involvement of energy change resulted by the NHC ligand conformation change during global structural optimizations. Note that in the optimization of open complexes, the alkane ring is "clipped off" into thioanisole and diphenyl(alkyl)phosphane, followed by full optimizations without geometric constraints. Ligands employed in closed and open complexes are denoted as *ligand(P+S)* and *ligand(P)+(S)*, respectively. The vdW interaction energy between two ligands in *ligand(P)+(S)*, namely thioanisole (*ligand (S)*) and diphenyl(alkyl)phosphane (*ligand (P)*), was also computed to obtain the energy directly associated with the ring formation/dissociation. The complex formation energy, non-covalent vdW interaction corrections and ring strain energy are defined as follows:

$E_{\text{closed complex formation}} = E_{\text{complex}} - E_{\text{PtCl2}} - E_{\text{ligand(P+S)}}$

$E_{\text{open complex formation}} = E_{\text{complex}} - E_{\text{PtCl2}} - E_{\text{ligand(P)}} - E_{\text{ligand(S)}} + E_{\text{vdW}}$

vdW interaction energy correction $E_{\text{vdW}} = E_{\text{ligand(P)+(S)}} - E_{\text{ligand(P)}} - E_{\text{ligand(S)}}$

Ring strain energy $E_{strain} = E_{\text{close complex formation}} - E_{\text{open complex formation}}$

Table S1. A series of DFT-D optimized closed/open ring configuration of *cis*-$PtCl_2$ complexes.

Bridge carbon number	Closed state	Open state	Energy difference between the two states (kcal/mol)
1	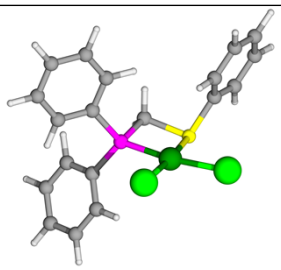 Calculated P-Pt-S angle: 73.92°	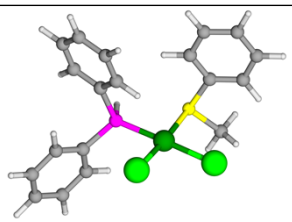	5.02

2	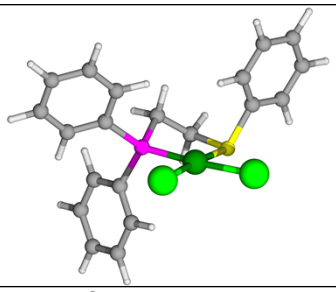	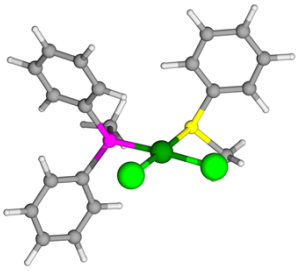	1.13
3	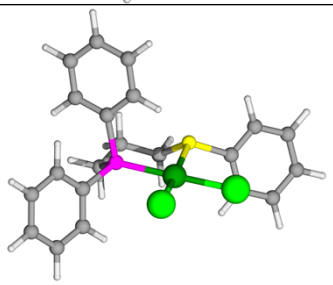	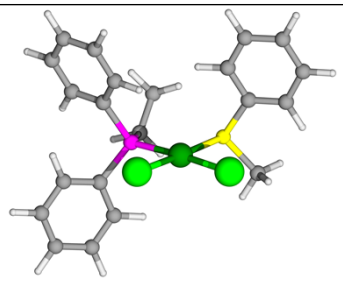 Calculated P-Pt-S angle: 87.45°	2.08
4	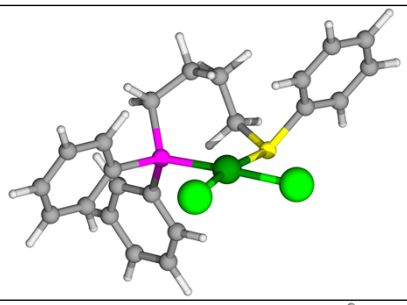	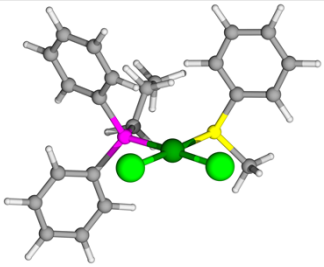	3.54
5	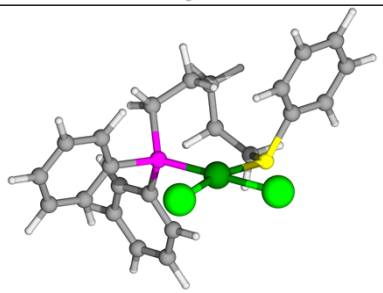 Calculated P-Pt-S angle: 98.06°	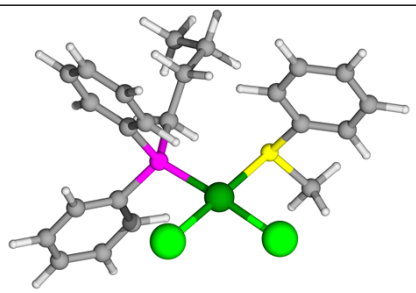	7.47

DFT-D optimized configuration of 4a, 5c and 4e complexes

Table S2. Atomic coordinates of **4a**.

Atom	x	y	z	Atom	x	y	z
Pt	6.291	13.101	9.566	C	8.164	14.652	11.410
S	8.225	12.808	10.932	H	7.654	14.717	12.381
P	7.084	15.227	10.018	H	9.168	15.094	11.464
N	4.395	10.761	9.625	C	3.506	17.660	11.649
N	4.091	14.559	7.910	H	2.625	18.192	12.014
N	3.379	12.802	8.965	C	7.808	11.895	12.401
N	6.413	9.973	9.520	C	7.848	9.852	9.332
C	5.711	11.156	9.444	H	8.175	10.631	8.631
C	4.508	13.587	8.796	H	8.074	8.861	8.916
C	4.302	9.395	9.854	H	8.381	9.980	10.285
H	3.357	8.889	10.020	C	3.790	16.365	12.103
C	3.365	11.733	9.927	H	3.124	15.877	12.821
H	3.568	12.166	10.931	C	9.446	18.240	8.465
H	2.384	11.239	9.908	H	9.826	19.216	8.775
C	5.785	16.292	10.702	C	6.472	11.756	12.830
C	5.568	8.903	9.778	H	5.678	12.221	12.233
H	5.930	7.885	9.864	C	8.636	17.510	9.336
C	2.300	13.288	8.239	H	8.392	17.915	10.321
H	1.321	12.820	8.245	C	8.555	10.558	14.281
C	4.912	15.683	11.634	H	9.363	10.083	14.842
H	5.098	14.655	11.954	C	4.362	18.268	10.718
C	8.853	11.294	13.136	H	4.146	19.275	10.351
H	9.886	11.405	12.795	C	7.224	10.419	14.714
C	2.752	14.391	7.584	H	7.000	9.845	15.615
H	2.237	15.069	6.913	C	5.490	17.592	10.245
C	4.919	15.615	7.353	H	6.135	18.073	9.507

H	4.853	16.528	7.958	C	9.781	17.728	7.202
H	4.591	15.826	6.326	H	10.416	18.306	6.528
H	5.958	15.275	7.334	C	6.190	11.021	13.978
C	8.497	15.730	7.686	H	5.152	10.916	14.308
H	8.145	14.731	7.409	C	9.310	16.462	6.821
C	8.131	16.248	8.944	H	9.586	16.041	5.851

Table S3. Atomic coordinates of **5c**.

Atom	x	y	z	Atom	x	y	z
Pt	12.425	13.075	14.056	H	14.235	9.735	10.922
P	13.099	12.394	11.958	C	17.372	10.572	11.954
S	11.549	9.729	7.325	H	18.384	10.163	11.988
N	10.239	11.241	14.880	C	9.423	12.447	14.952
N	13.678	14.712	13.826	H	8.410	12.182	15.280
N	10.012	13.402	15.851	H	9.414	12.911	13.947
N	11.589	14.641	16.679	C	14.132	15.672	13.300
N	12.008	10.036	14.555	C	12.104	10.998	9.657
C	11.583	11.347	14.593	H	11.839	11.939	9.155
C	10.954	9.161	14.801	H	13.156	10.807	9.393
H	11.083	8.084	14.820	C	13.164	13.691	10.669
C	15.815	12.369	12.434	C	11.228	9.869	9.115
H	15.613	13.351	12.865	H	11.465	8.910	9.601
C	11.946	11.166	11.171	H	10.164	10.096	9.283
H	12.070	10.212	11.708	C	16.325	9.820	11.407
H	10.938	11.527	11.422	H	16.517	8.822	11.005
C	17.110	11.852	12.463	C	12.064	14.564	10.569
H	17.918	12.446	12.898	H	11.251	14.477	11.297
C	13.404	9.646	14.441	C	12.029	15.541	9.573

H	14.004	10.564	14.458	H	11.163	16.203	9.491
H	13.595	9.119	13.498	C	10.634	8.022	5.446
H	13.688	9.003	15.288	H	11.430	8.464	4.841
C	9.842	9.920	15.015	C	9.439	7.877	7.553
H	8.819	9.632	15.237	H	9.281	8.186	8.586
C	9.652	13.674	17.169	C	13.108	15.682	8.687
H	8.723	13.335	17.616	H	13.089	16.457	7.919
C	10.636	14.466	17.674	C	14.196	16.746	12.313
H	10.717	14.940	18.646	H	14.646	16.356	11.387
C	11.255	13.943	15.532	H	14.804	17.590	12.666
C	14.756	11.626	11.872	H	13.180	17.102	12.071
C	12.864	15.308	16.879	C	14.210	14.820	8.790
H	12.758	16.056	17.675	H	15.050	14.922	8.097
H	13.163	15.802	15.949	C	10.459	8.452	6.776
H	13.647	14.582	17.150	C	8.614	6.889	7.002
C	14.236	13.822	9.768	H	7.827	6.448	7.618
H	15.091	13.145	9.834	C	9.803	7.042	4.907
C	15.028	10.343	11.361	H	9.952	6.724	3.872
H	8.133	5.704	5.254	C	8.784	6.470	5.680
H	8.133	5.704	5.254				

Table S4. Atomic coordinates of **4e**.

Atom	x	y	z	Atom	x	y	z
Pt	8.137	13.054	5.440	C	11.165	14.862	6.169
P	6.395	14.498	5.861	H	10.407	14.331	6.747
S	9.446	14.512	3.990	C	4.662	12.628	9.080
N	5.830	10.913	5.542	H	4.974	12.356	10.091
N	9.646	11.084	7.150	C	11.461	11.926	4.177
N	7.295	10.772	7.119	H	10.641	12.069	3.460

C	7.050	11.418	5.928	H	12.160	11.180	3.784
C	9.783	11.931	6.056	H	11.988	12.877	4.315
C	5.203	11.171	4.259	C	3.880	13.317	6.490
H	5.510	12.157	3.910	H	3.568	13.584	5.479
H	4.112	11.158	4.378	C	5.023	14.809	2.004
H	5.510	10.416	3.518	H	5.302	14.376	1.040
N	10.919	11.440	5.435	C	5.519	13.368	8.266
C	5.739	14.467	3.150	H	6.508	13.649	8.640
H	6.581	13.767	3.097	C	4.337	15.929	4.482
C	5.409	15.013	4.403	H	4.052	16.364	5.444
C	3.414	12.213	8.600	C	8.512	17.520	5.503
H	2.753	11.613	9.229	H	8.054	18.500	5.725
C	10.929	15.117	4.812	H	9.600	17.697	5.460
C	5.141	13.723	6.956	C	11.422	10.330	6.100
C	6.270	9.909	7.463	H	12.322	9.820	5.773
H	6.270	9.339	8.387	C	11.933	15.724	4.033
C	6.767	16.087	6.805	H	11.781	15.872	2.962
H	6.030	16.859	6.530	C	3.025	12.565	7.302
H	6.567	15.815	7.851	H	2.050	12.255	6.917
C	8.442	11.147	7.932	C	13.142	16.097	4.625
H	8.511	10.475	8.796	H	13.917	16.560	4.010
H	8.302	12.199	8.248	C	12.377	15.235	6.752
C	7.987	17.087	4.128	H	12.545	15.026	7.811
H	7.911	17.986	3.489	C	3.952	15.711	2.093
H	6.958	16.723	4.222	H	3.384	15.981	1.200
C	10.614	10.084	7.165	C	13.372	15.856	5.986
H	10.664	9.321	7.932	H	14.325	16.139	6.439
C	8.212	16.581	6.681	C	3.615	16.265	3.336
H	8.488	17.111	7.607	H	2.778	16.965	3.409

H	8.865	15.698	6.643	C	8.792	16.099	3.287
C	5.347	9.999	6.470	H	9.695	16.578	2.883
H	4.377	9.525	6.370	H	8.182	15.763	2.436

Crystallographic Information

Table S5. Crystallographic Data for **5a**.

Compound name	**5a**
Empirical formula	$C_{30}H_{32}B_2F_8N_5PPtS$
Formula weight	894.34
Temperature / K	100.0(2)
Crystal system	triclinic
Space group	P -1
a/Å, b/Å, c/Å	11.57930(12), 11.85721(14), 13.18425(17)
α/°, β/°, γ/°	101.9598(10), 103.360(1), 103.1011(10)
Volume / Å^3	1649.68(4)
Z	2
ρcalc / mg mm^{-3}	1.801
μ / mm^{-1}	4.441
F(000)	876
Crystal size / mm^3	0.173 × 0.086 × 0.015
2Θ range for data collection	2.738 to 33.897
Index ranges	-18≤h≤17-17≤k≤18,-19≤l≤20
Reflections collected	106307
Independent reflections	106307[R(int) = 0.0605]
Data/restraints/parameters	106307/53/483
Goodness-of-fit on F2	1.042
Final R indexes [I>2σ (I)]	R1 = 0.0409, wR2 = 0.1029
Final R indexes [all data]	R1 = 0.0513, wR2 = 0.1069
Largest diff. peak/hole / e Å^{-3}	5.392/-1.455

Table S6. Crystallographic Data for **4b**.

Compound name	**4b**
Empirical formula	$C_{29}H_{31}B_2F_8N_4PPtS$
Formula weight	867.32
Temperature / K	99.98(10)
Crystal system	monoclinic
Space group	P 1 21/c 1
a/Å, b/Å, c/Å	10.1155(2), 20.5747(4), 15.5888(3)
α/°, β/°, γ/°	90, 94.137(2), 90
Volume / $Å^3$	3235.94(11)
Z	4
ρcalc / mg mm^{-3}	1.780
μ / mm^{-1}	4.524
F(000)	1696
Crystal size / mm^3	0.387 × 0.105 × 0.067
2Θ range for data collection	1.980 to 31.060
Index ranges	$-14\leq h\leq 12$, $-25\leq k\leq 25$, $-20\leq l\leq 21$
Reflections collected	37346
Independent reflections	8342[R(int) = 0.0378]
Data/restraints/parameters	8342/0/417
Goodness-of-fit on F2	1.060
Final R indexes [I>2σ (I)]	R1 = 0.0299, wR2 = 0.0723
Final R indexes [all data]	R1 = 0.0407, wR2 = 0.0766
Largest diff. peak/hole / e $Å^{-3}$	3.864/-0.605

Table S7. Crystallographic Data for **6b**.

Compound name	**6b**
Empirical formula	$C_{29}H_{31}BClF_4N_4PPtS$
Formula weight	815.96
Temperature / K	100.0(2)
Crystal system	triclinic
Space group	P -1
a/Å, b/Å, c/Å	9.19990(10), 10.8797(2), 20.6779(3)
α/°, β/°, γ/°	95.5090(10), 100.6030(10), 112.4480(10)
Volume / $Å^3$	1848.45(5)
Z	2
ρcalc / mg mm^{-3}	1.466
μ / mm^{-1}	4.010
F(000)	800
Crystal size / mm^3	0.233 × 0.115 × 0.022
2Θ range for data collection	2.433 to 33.956
Index ranges	-14≤h≤13, -17≤k≤16, -32≤l≤30
Reflections collected	115173
Independent reflections	13578[R(int) = 0.0628]
Data/restraints/parameters	13578/176/519
Goodness-of-fit on F2	1.071
Final R indexes [I>2σ (I)]	R1 = 0.0568, wR2 = 0.1092
Final R indexes [all data]	R1 = 0.0775, wR2 = 0.1150
Largest diff. peak/hole / e $Å^{-3}$	2.482/-2.241

Table S8. Crystallographic Data for **4c**.

Compound name	**4c**
Empirical formula	$C_{32}H_{36}B_2F_8N_5PPtS$
Formula weight	922.40
Temperature / K	100.00(10)
Crystal system	orthorhombic
Space group	P n a 21
a/Å, b/Å, c/Å	20.6049(6), 19.1262(6), 8.8690(3)
α/°, β/°, γ/°	90, 90, 90
Volume / Å^3	3495.22(19)
Z	4
ρcalc / mg mm^{-3}	1.753
μ / mm^{-1}	4.195
F(000)	1816
Crystal size / mm^3	0.319 × 0.035 × 0.033
2Θ range for data collection	2.130 to 32.309
Index ranges	-27≤h≤30, -27≤k≤24, -12≤l≤10
Reflections collected	45647
Independent reflections	9617[R(int) = 0.0541]
Data/restraints/parameters	9617/1/455
Goodness-of-fit on F2	1.083
Final R indexes [I>2σ (I)]	R1 = 0.0346, wR2 = 0.0779
Final R indexes [all data]	R1 = 0.0543, wR2 = 0.0909
Largest diff. peak/hole / e Å^{-3}	2.825/-1.823

Table S9. Crystallographic Data for **4d**.

Compound name	**4d**
Empirical formula	$C_{32}H_{37}B_2Cl_2F_8N_4PPtS$
Formula weight	980.29
Temperature / K	100.1(3)
Crystal system	monoclinic
Space group	P 1 21/c 1
a/Å, b/Å, c/Å	12.1158(6), 16.2810(6), 18.5842(8)
α/°, β/°, γ/°	90, 96.055(4), 90
Volume / $Å^3$	3645.4(3)
Z	4
ρcalc / mg mm^{-3}	1.786
μ / mm^{-1}	4.169
F(000)	1928
Crystal size / mm^3	0.262 × 0.069 × 0.049
2Θ range for data collection	2.103 to 38.156
Index ranges	-20≤h≤20, -24≤k≤28, -31≤l≤31
Reflections collected	65750
Independent reflections	18728[R(int) = 0.1402]
Data/restraints/parameters	18728/0/462
Goodness-of-fit on F2	1.021
Final R indexes [I>2σ (I)]	R1 = 0.0817, wR2 = 0.1839
Final R indexes [all data]	R1 = 0.1703, wR2 = 0.2236
Largest diff. peak/hole / e $Å^{-3}$	7.443/-4.865

Table S10. Crystallographic Data for **5d**.

Compound name	**5d**
Empirical formula	$C_{33}H_{38}B_2F_8N_5PPtS$
Formula weight	936.42
Temperature / K	113(19)
Crystal system	triclinic
Space group	P -1
a/Å, b/Å, c/Å	10.3866(2), 12.6158(2), 15.7425(3)
α/°, β/°, γ/°	68.424(2), 79.210(2), 73.111(2)
Volume / $Å^3$	1828.04(7)
Z	2
ρcalc / mg mm^{-3}	1.701
μ / mm^{-1}	4.012
F(000)	924
Crystal size / mm^3	0.510 × 0.350 × 0.150
2Θ range for data collection	2.327 to 30.913
Index ranges	$-14\leq h\leq 13$, $-17\leq k\leq 18$, $-21\leq l\leq 21$
Reflections collected	40669
Independent reflections	9492[R(int) = 0.0979]
Data/restraints/parameters	9492/0/463
Goodness-of-fit on F2	1.172
Final R indexes [I>2σ (I)]	R1 = 0.0415, wR2 = 0.1108
Final R indexes [all data]	R1 = 0.0450, wR2 = 0.1122
Largest diff. peak/hole / e $Å^{-3}$	3.585/-3.985

Table S11. Crystallographic Data for **5e**.

Compound name	**5e**
Empirical formula	$C_{34}H_{40}B_2F_8N_5PPtS$
Formula weight	950.45
Temperature / K	125(30)
Crystal system	triclinic
Space group	P -1
a/Å, b/Å, c/Å	10.6014(2), 12.7257(3), 16.4959(3)
α/°, β/°, γ/°	70.981(2), 72.466(2), 67.598(2)
Volume / Å^3	1904.86(8)
Z	2
ρcalc / mg mm^{-3}	1.657
μ / mm^{-1}	3.851
F(000)	940
Crystal size / mm^3	0.100 × 0.100 × 0.100
2Θ range for data collection	1.954 to 33.847
Index ranges	-16≤h≤15, -19≤k≤19, -24≤l≤25
Reflections collected	39457
Independent reflections	13292[R(int) = 0.1561]
Data/restraints/parameters	13292/0/472
Goodness-of-fit on F2	1.047
Final R indexes [I>2σ (I)]	R1 = 0.0767, wR2 = 0.1984
Final R indexes [all data]	R1 = 0.0855, wR2 = 0.2087
Largest diff. peak/hole / e Å^{-3}	5.891/-7.467

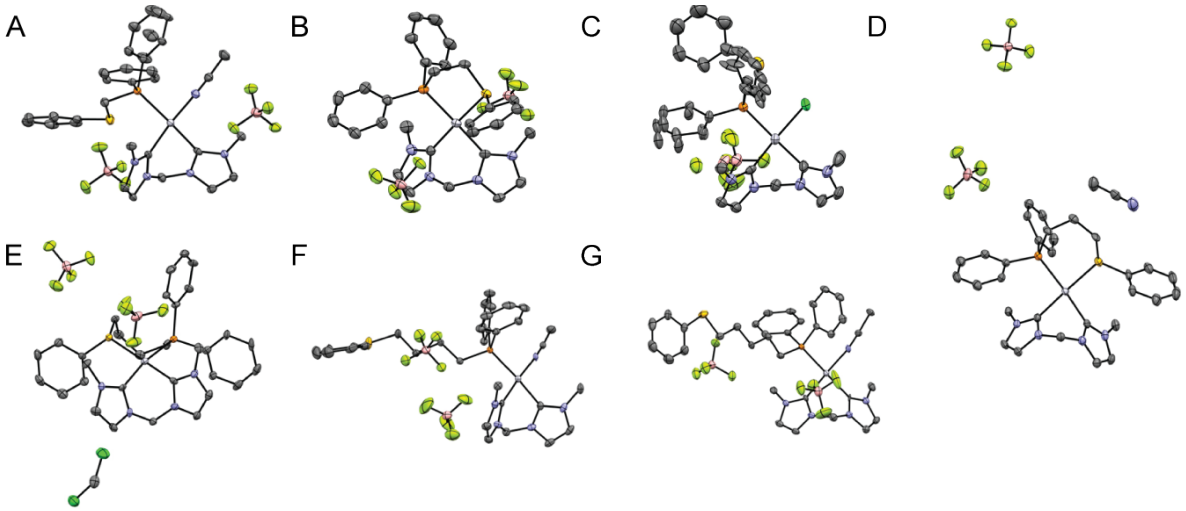

Figure S10. Crystal structures of A. **5a**, B. **4b**, C. **6b**, D. **4c**, E. **4d**, F. **5d**, and G. **5e** drawn in 50% probability thermal ellipsoids. Hydrogens and solvent molecules are omitted for clarity (C: gray, P: orange, S: yellow, N: purple, Pt: white, Cl: green, F: yellow-green, B: pink).

NMR Spectra

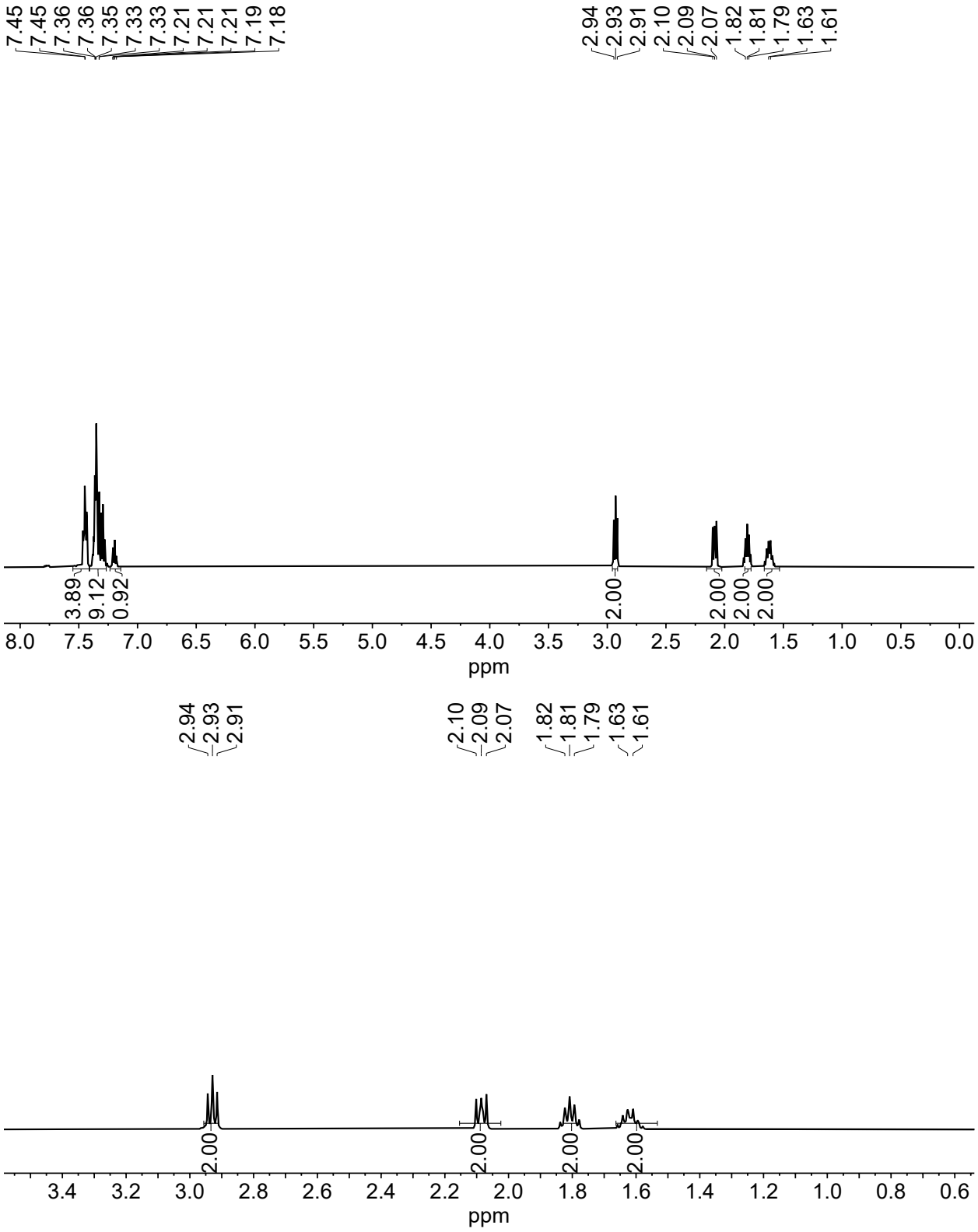

Figure S11. ^{1}H NMR (500 MHz, $CDCl_3$) spectrum of **7d** with expanded aliphatic region.

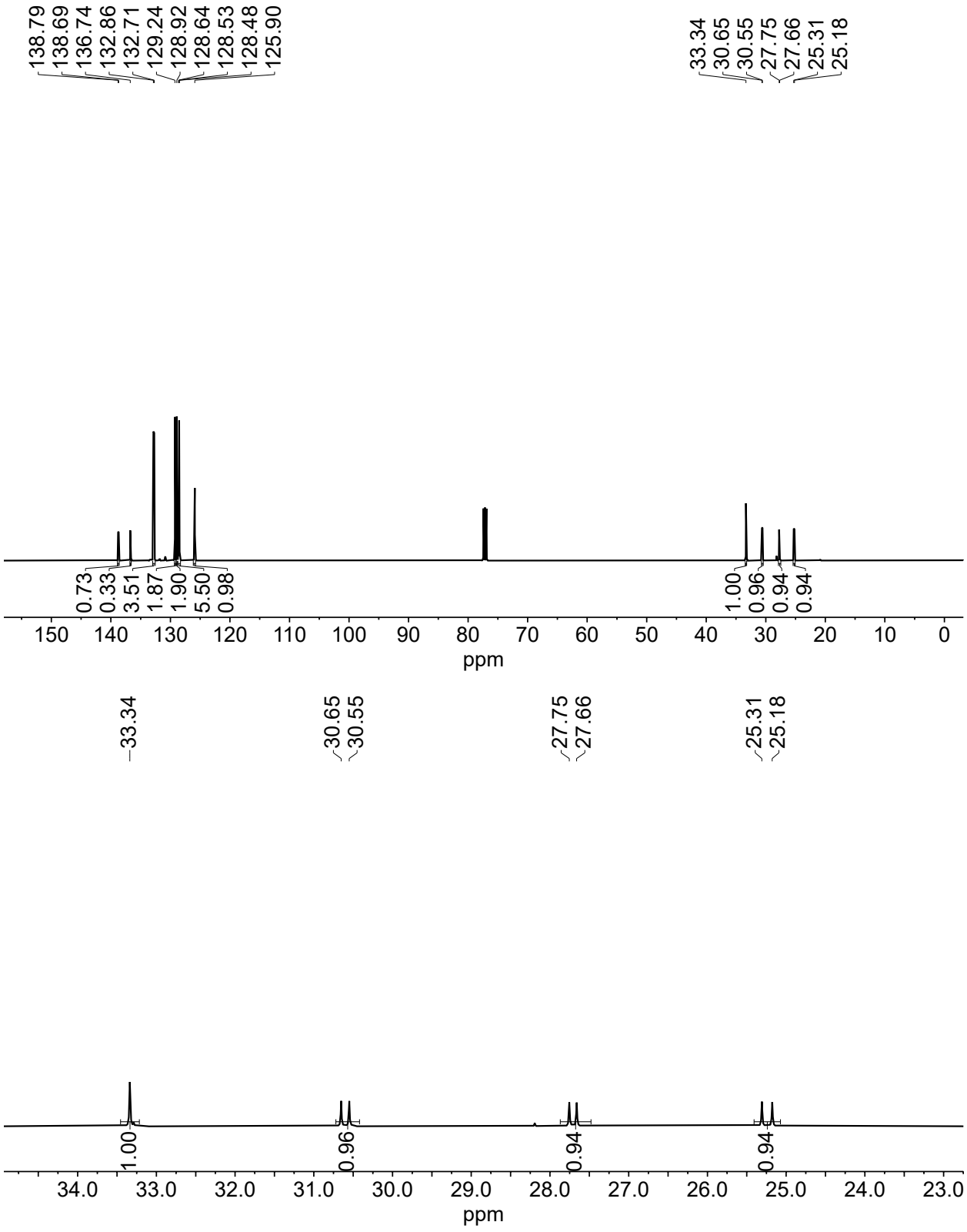

Figure S12. ^{13}C NMR (126 MHz, $CDCl_3$) spectrum of **7d** with expanded aliphatic region.

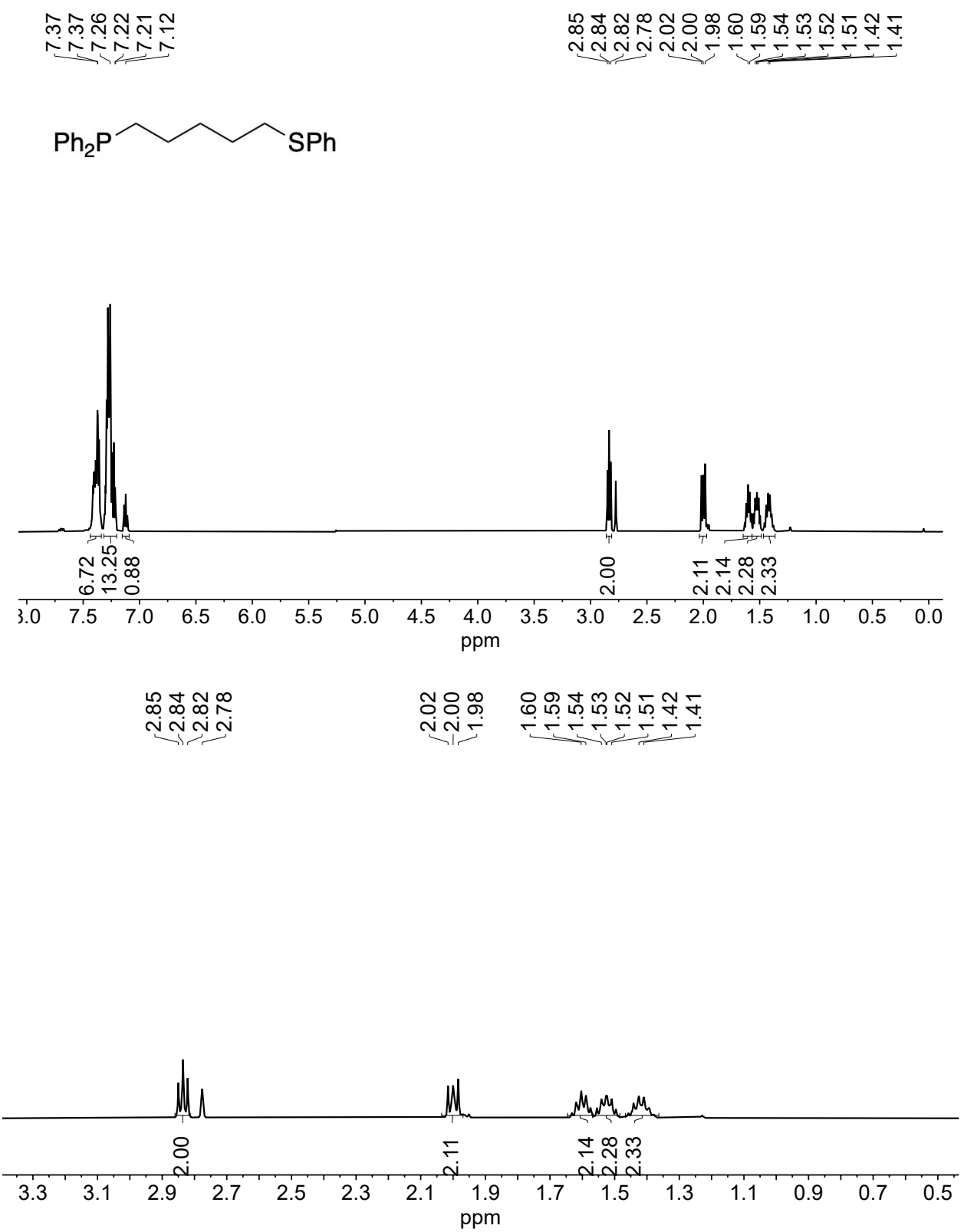
7.37
7.37
7.26
7.22
7.21
7.12
2.85
2.84
2.82
2.78
2.02
2.00
1.98
1.60
1.59
1.54
1.53
1.52
1.51
1.42
1.41
Ph2P
SPh
6.72
13.25
0.88
2.00
2.11
2.14
2.28
2.33
ppm
2.85
2.84
2.82
2.78
2.02
2.00
1.98
1.60
1.59
1.54
1.53
1.52
1.51
1.42
1.41
2.00
2.11
2.14
2.28
2.33
ppm

Figure S13. ^{1}H NMR (500 MHz, $CDCl_3$) spectrum of **7e** with expanded aliphatic region.

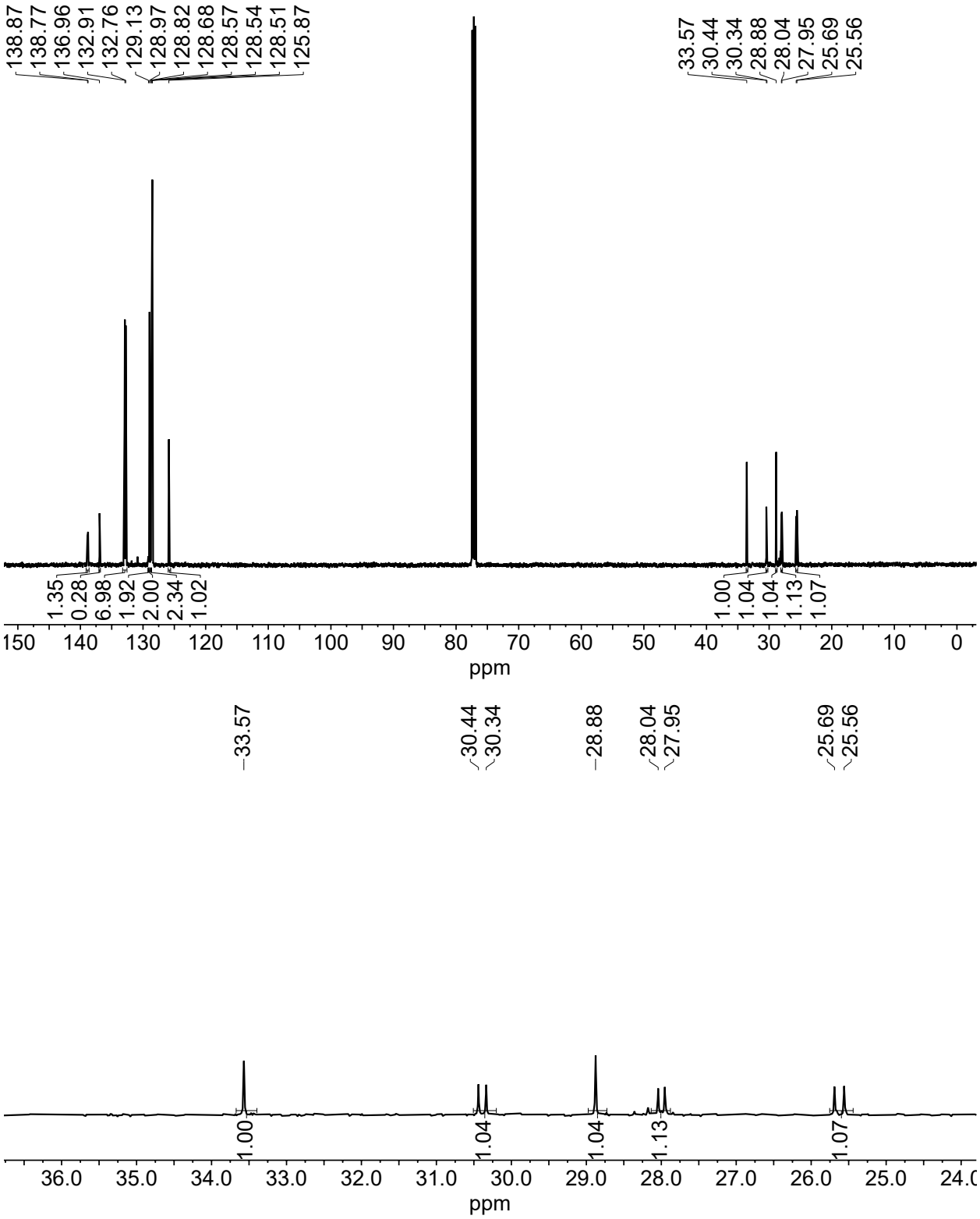

Figure S14. ^{13}C NMR (126 MHz, $CDCl_3$) spectrum of **7e** with expanded aliphatic region.

Solvent impurities[11] and residual effectors (nBu$_4$NCl) are marked accordingly.

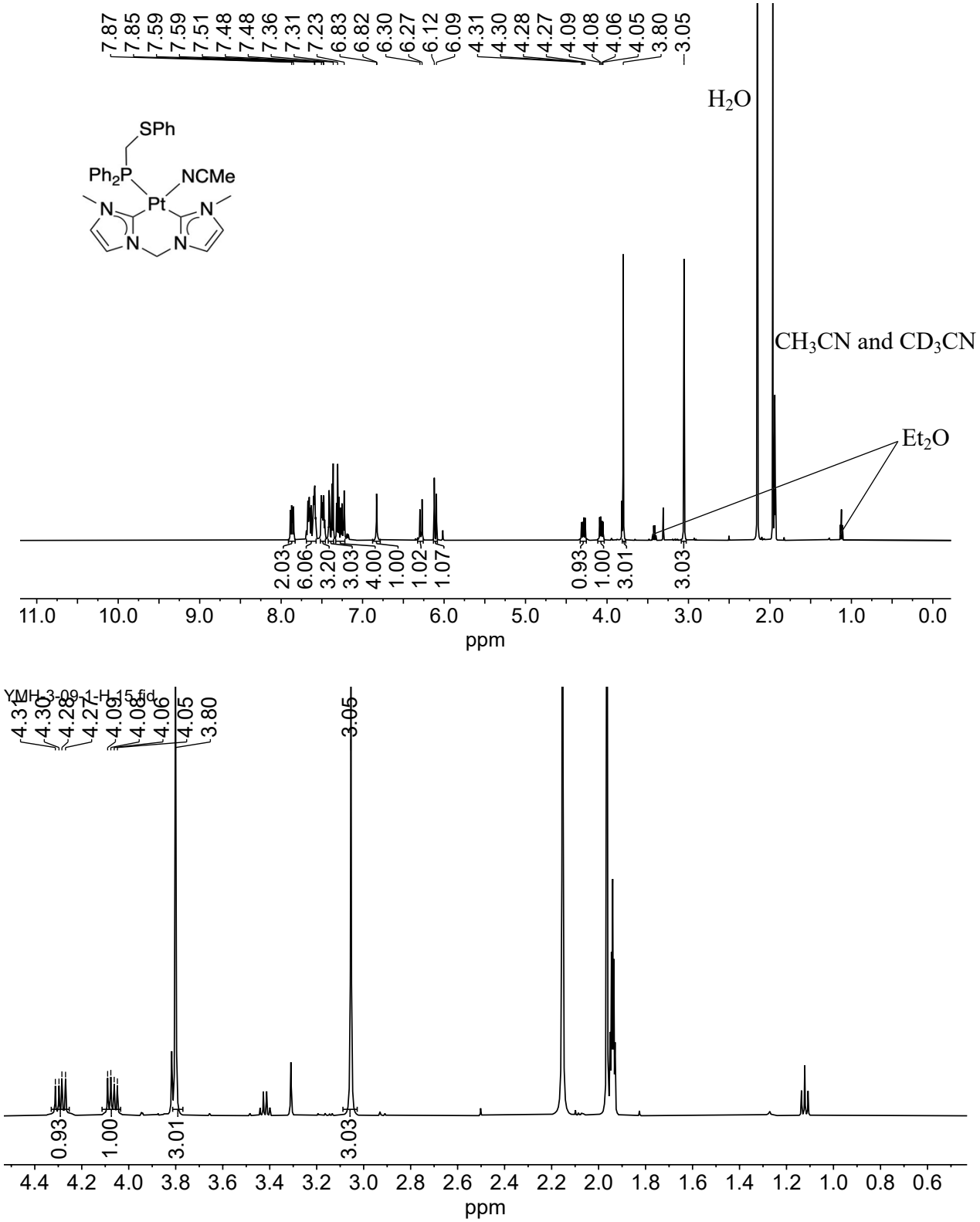

Figure S15. ^{1}H NMR (500 MHz, CD_3CN) spectrum of **5a** with expanded aliphatic region.

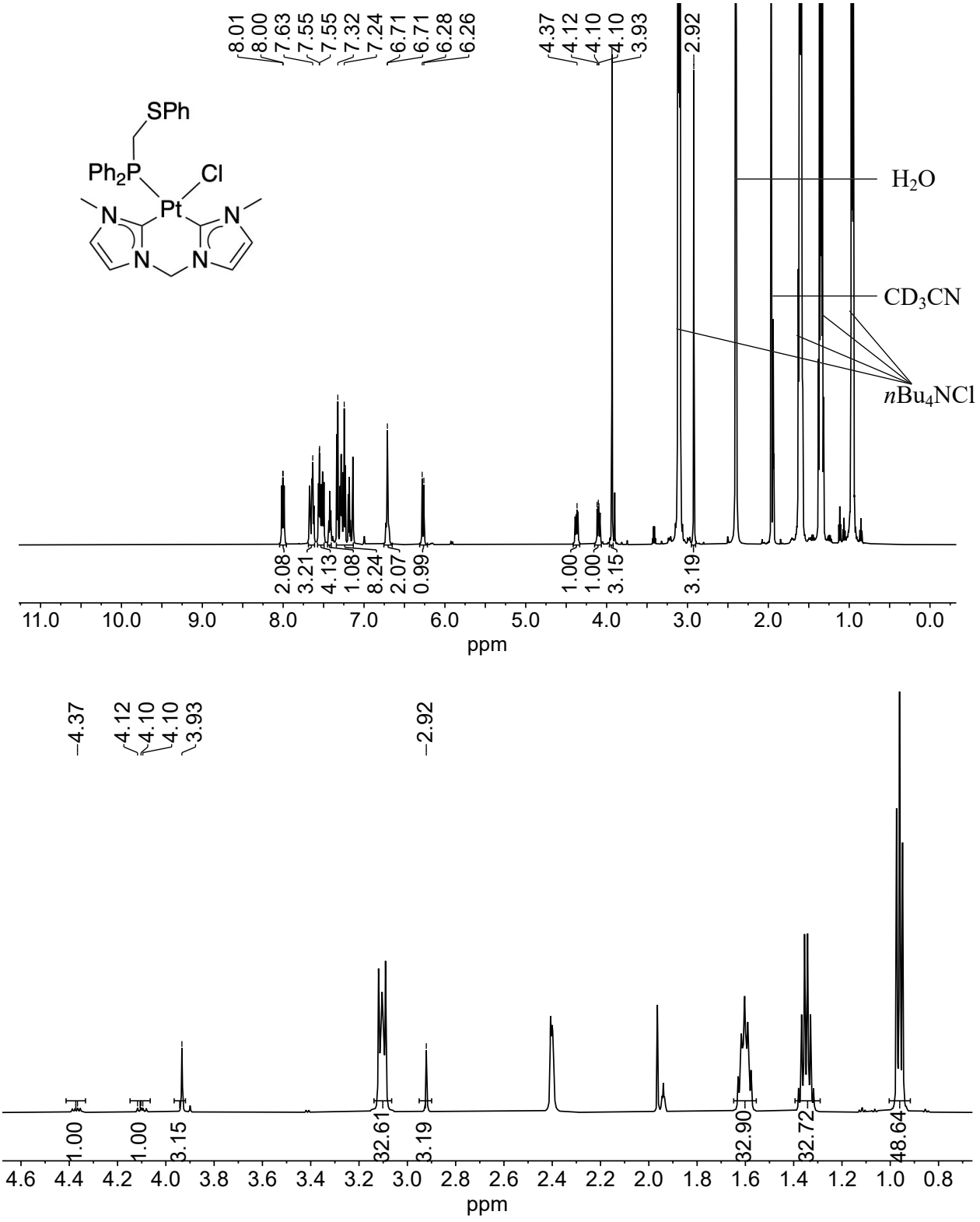
8.01
8.00
7.63
7.55
7.55
7.32
7.24
6.71
6.71
6.28
6.26
4.37
4.12
4.10
4.10
3.93
2.92
SPh
Ph2P
Cl
Pt
N
N
N
N
N
H2O
CD3CN
nBu4NCl
2.08
3.21
4.13
1.08
8.24
2.07
0.99
1.00
1.00
3.15
3.19
11.0
10.0
9.0
8.0
7.0
6.0
5.0
4.0
3.0
2.0
1.0
0.0
ppm
4.37
4.12
4.10
4.10
3.93
2.92
1.00
1.00
3.15
32.61
3.19
32.90
32.72
48.64
4.6
4.4
4.2
4.0
3.8
3.6
3.4
3.2
3.0
2.8
2.6
2.4
2.2
2.0
1.8
1.6
1.4
1.2
1.0
0.8
ppm

Figure S16. ^{1}H NMR (600 MHz, CD_3CN) spectrum of **6a** with expanded aliphatic region (excess nBu$_4$NCl).

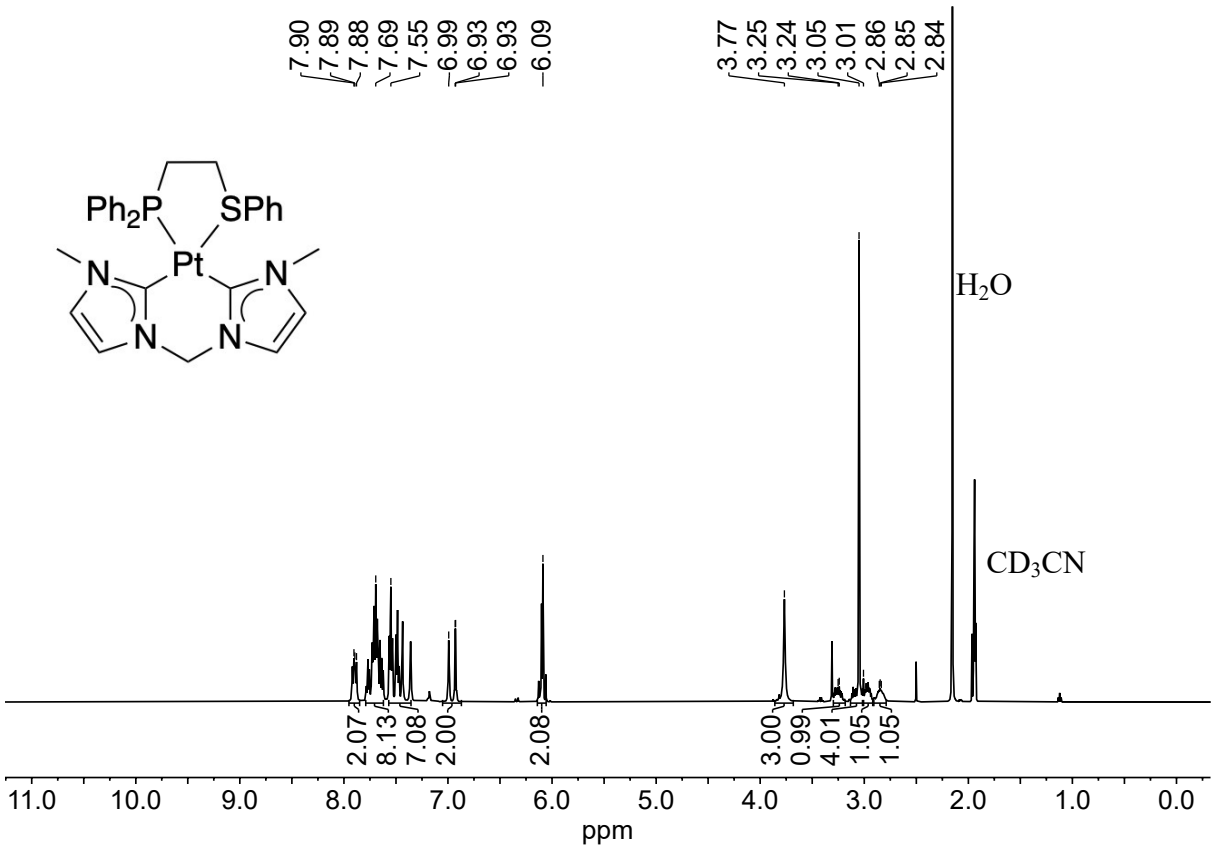

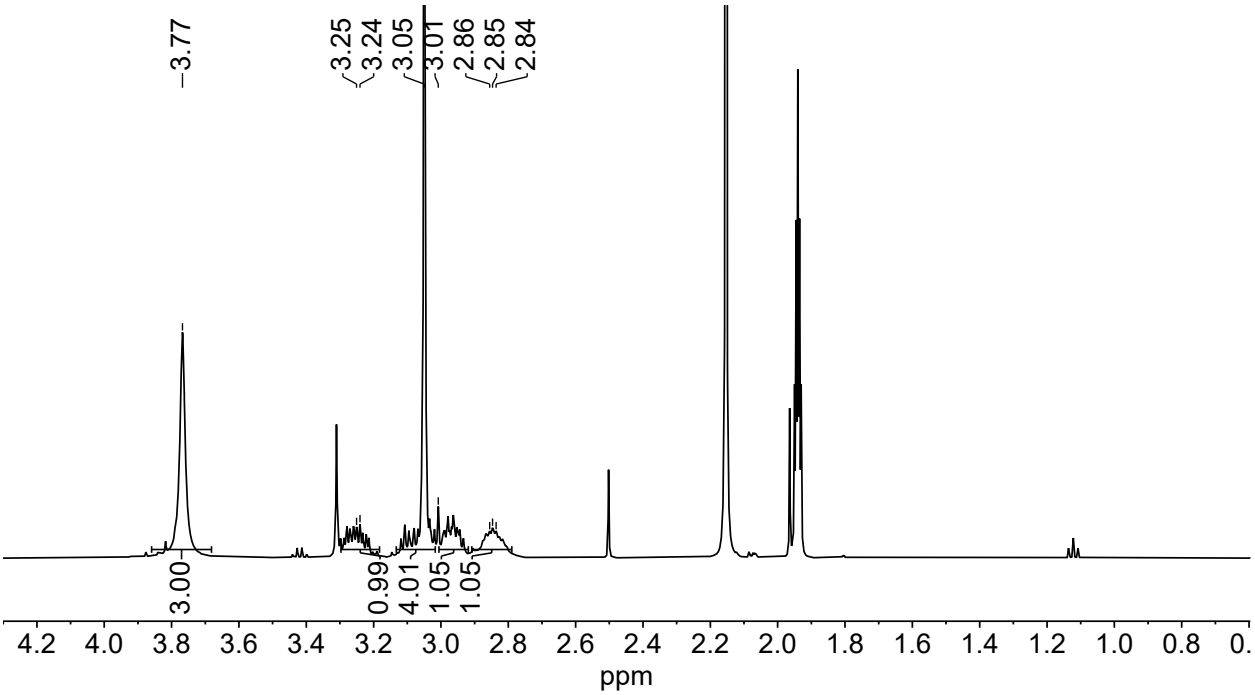

Figure S17. ^{1}H NMR (500 MHz, CD_3CN) spectrum of **4b** with expanded aliphatic region.

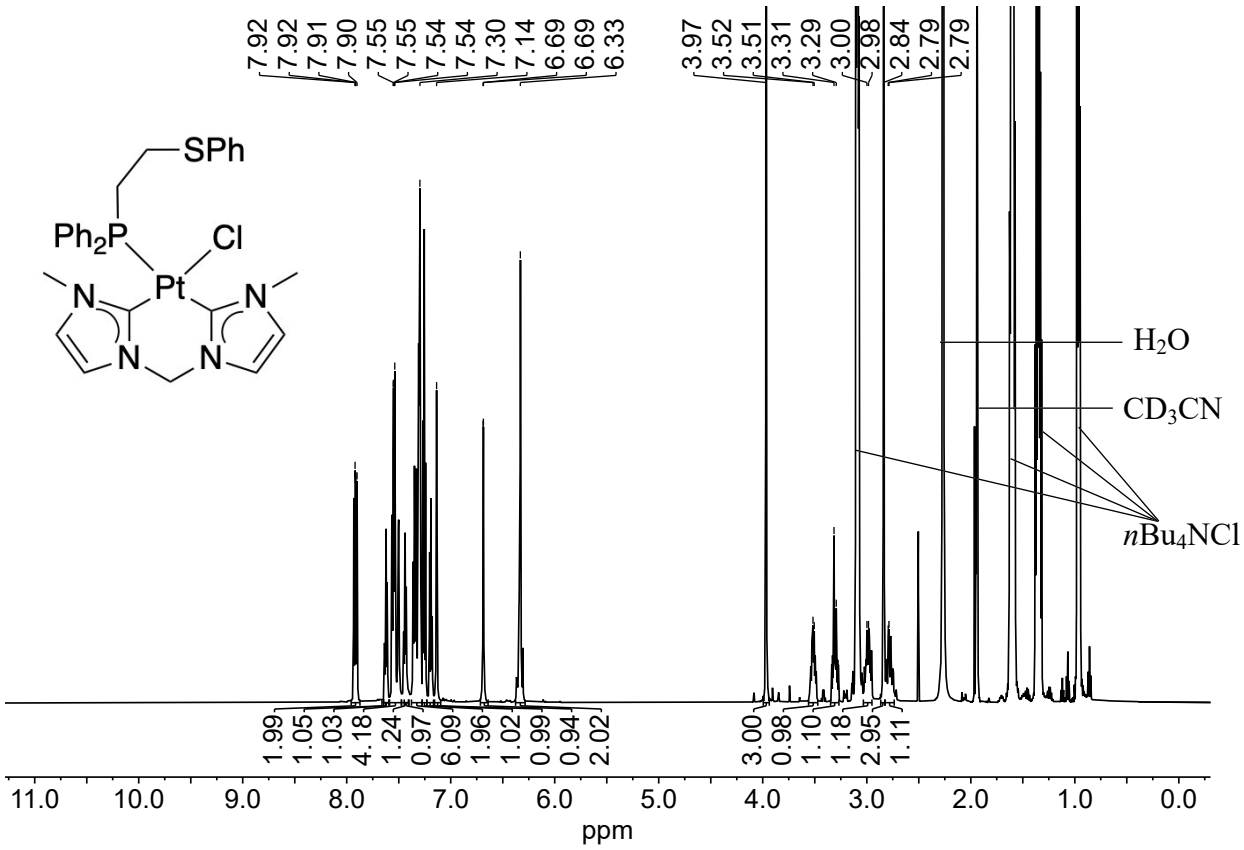

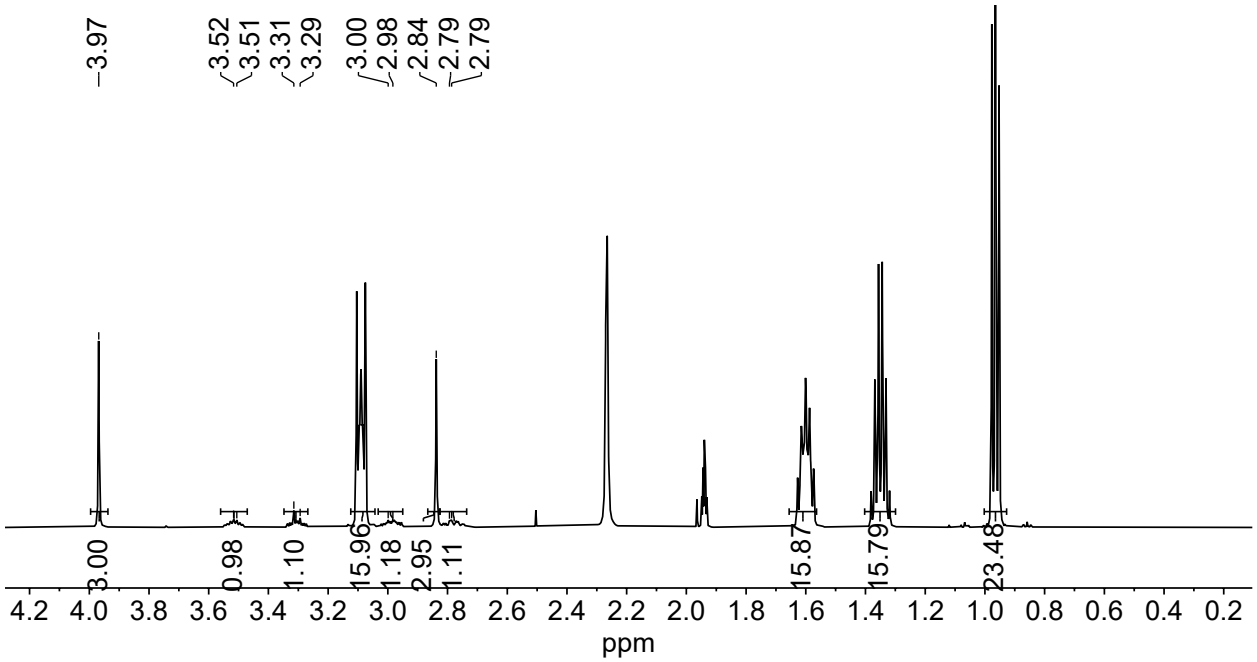

Figure S18. ^{1}H NMR (600 MHz, CD_3CN) spectrum of **6b** with expanded aliphatic region (excess nBu$_4$NCl).

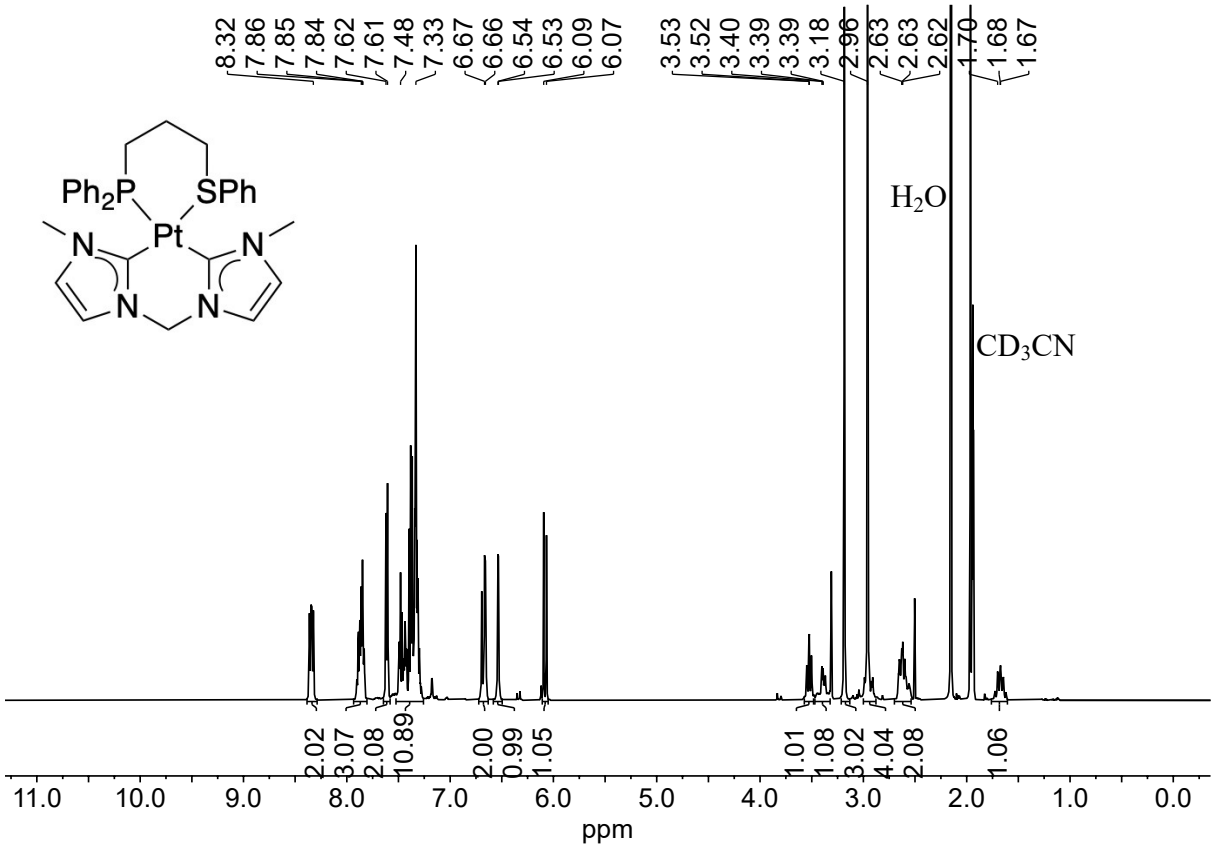

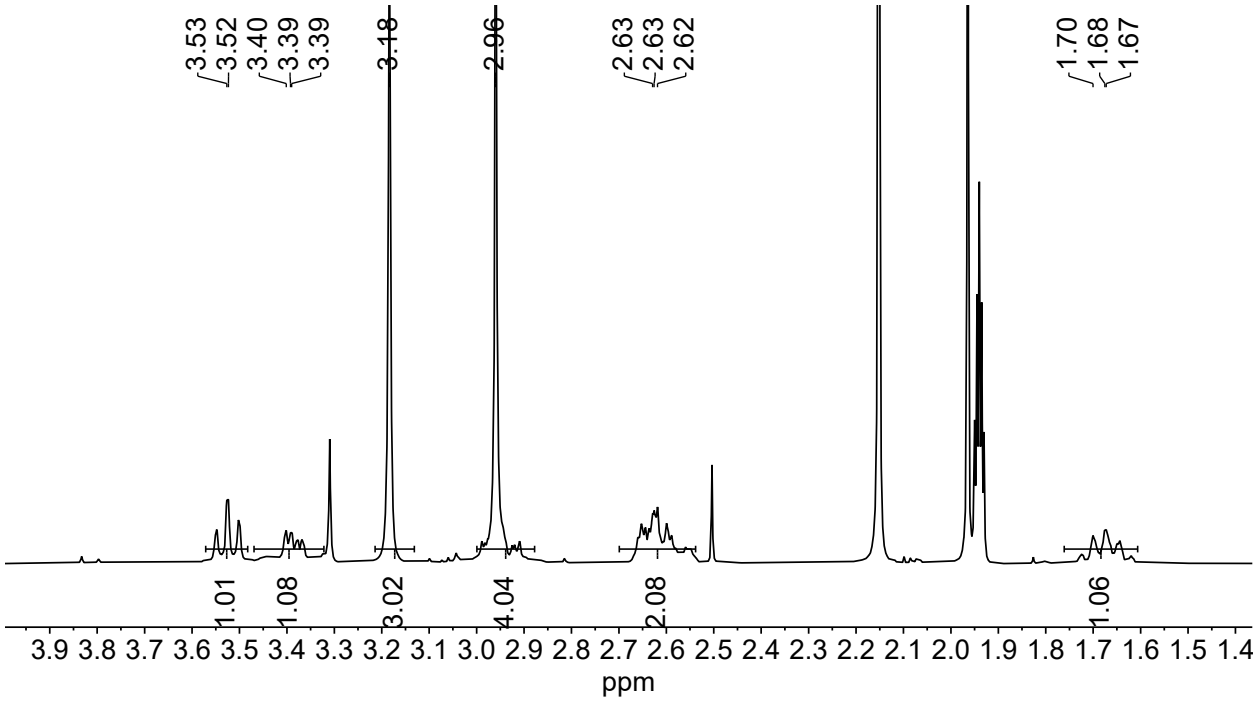

Figure S19. ^{1}H NMR (500 MHz, CD_3CN) spectrum of **4c** with expanded aliphatic region.

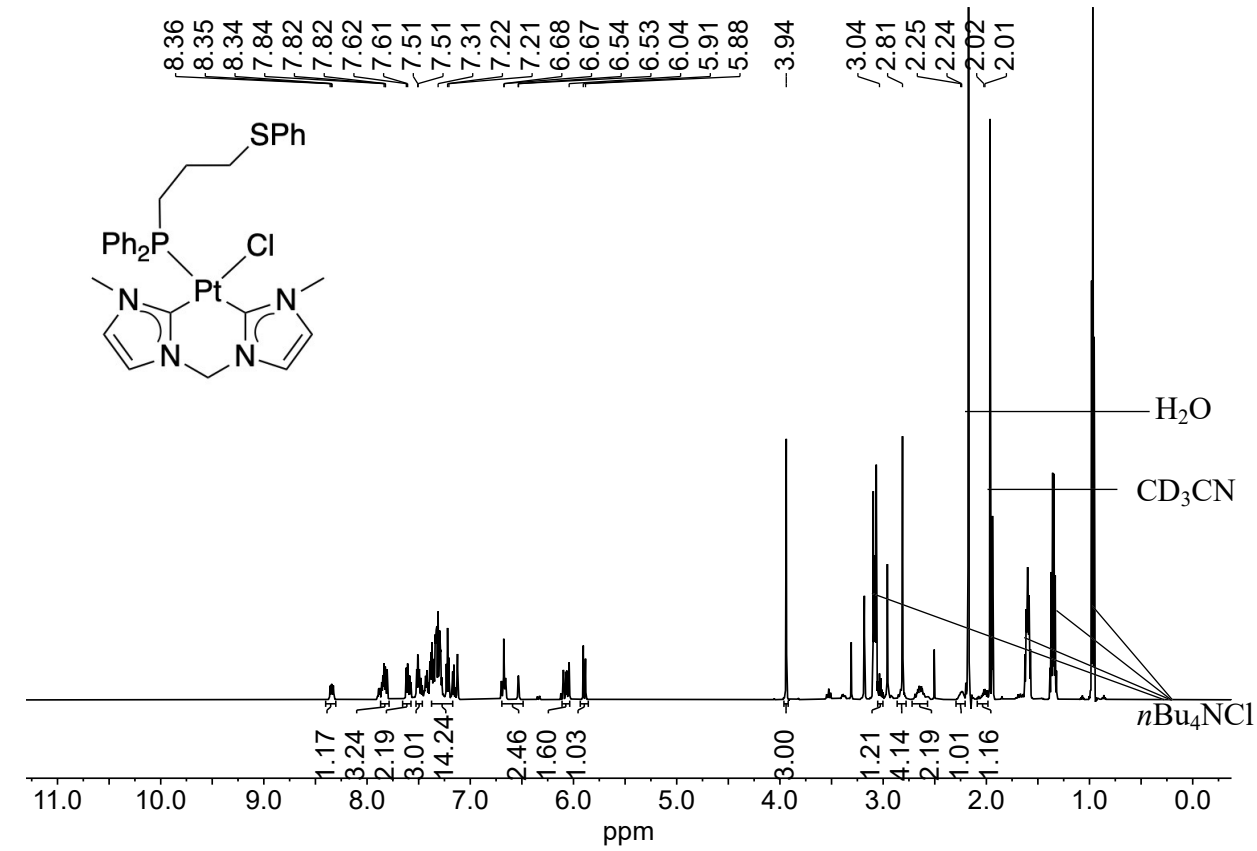

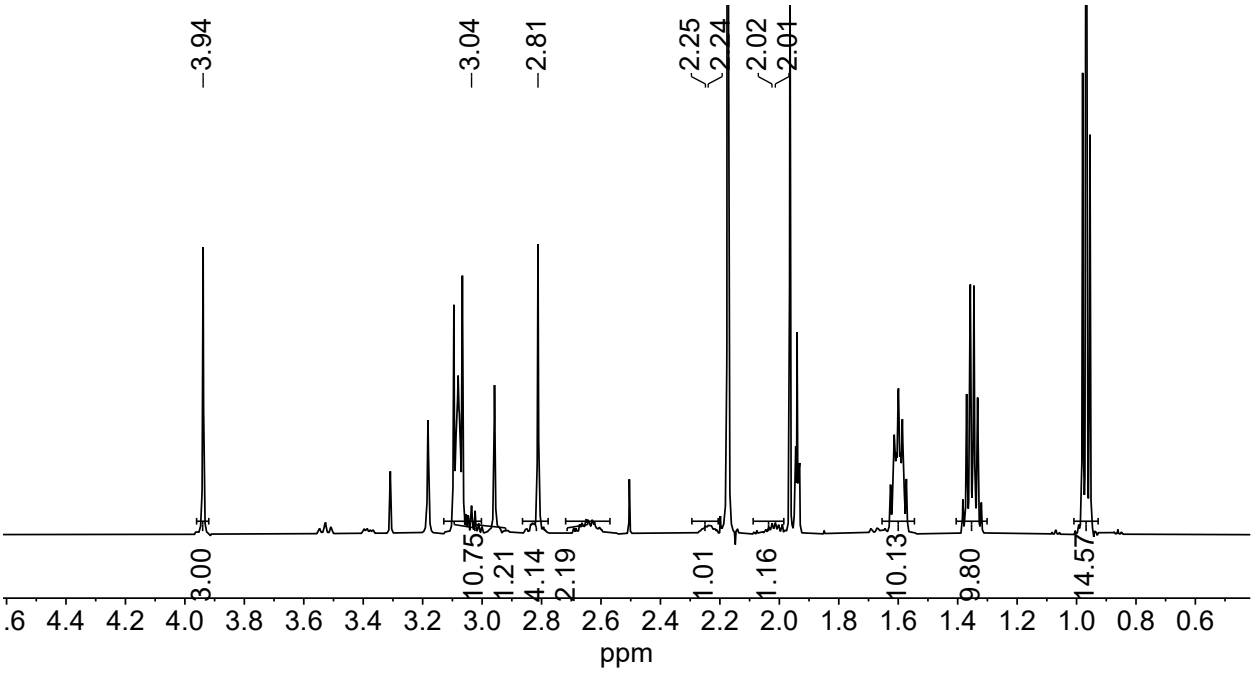

Figure S20. ^{1}H NMR (600 MHz, CD_3CN) spectrum of **6c** with expanded aliphatic region (excess nBu$_4$NCl).

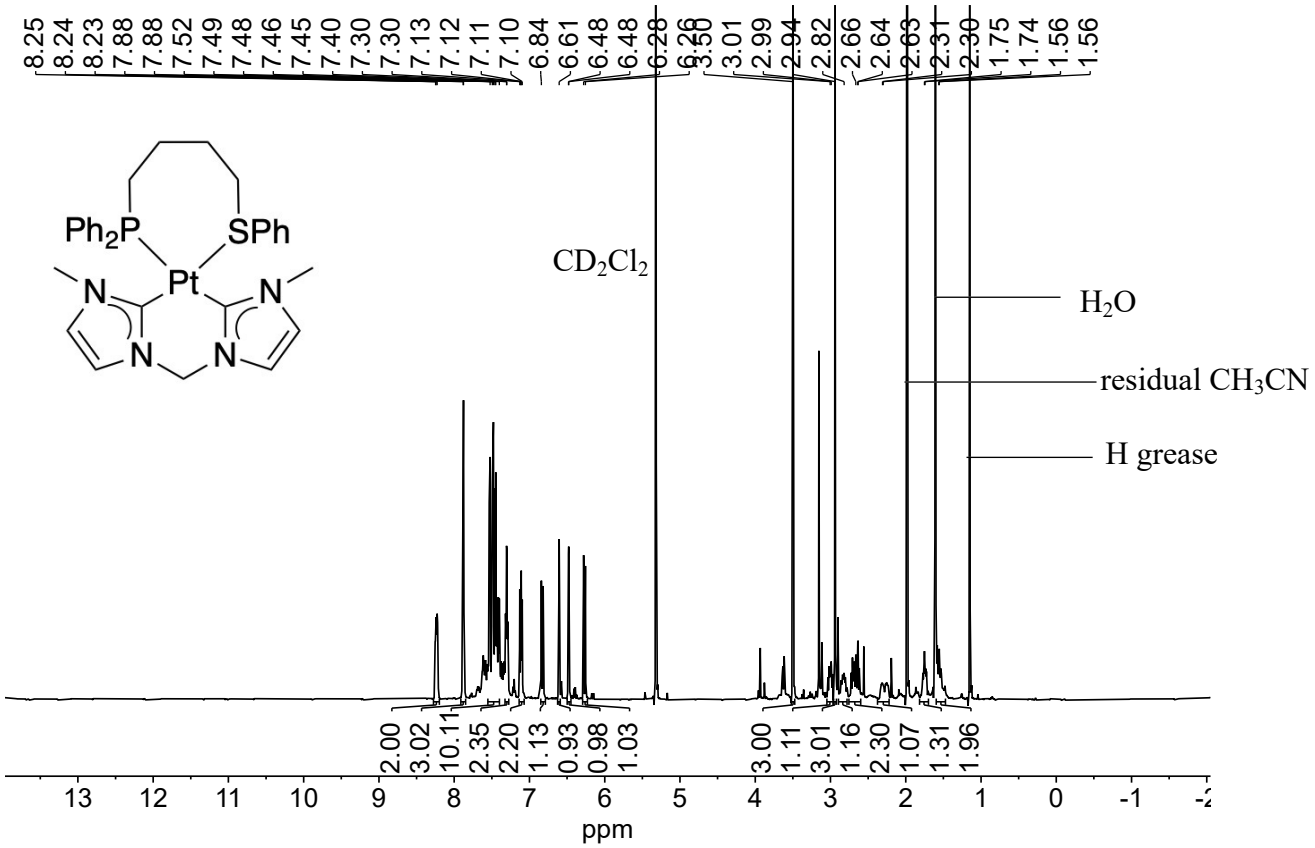

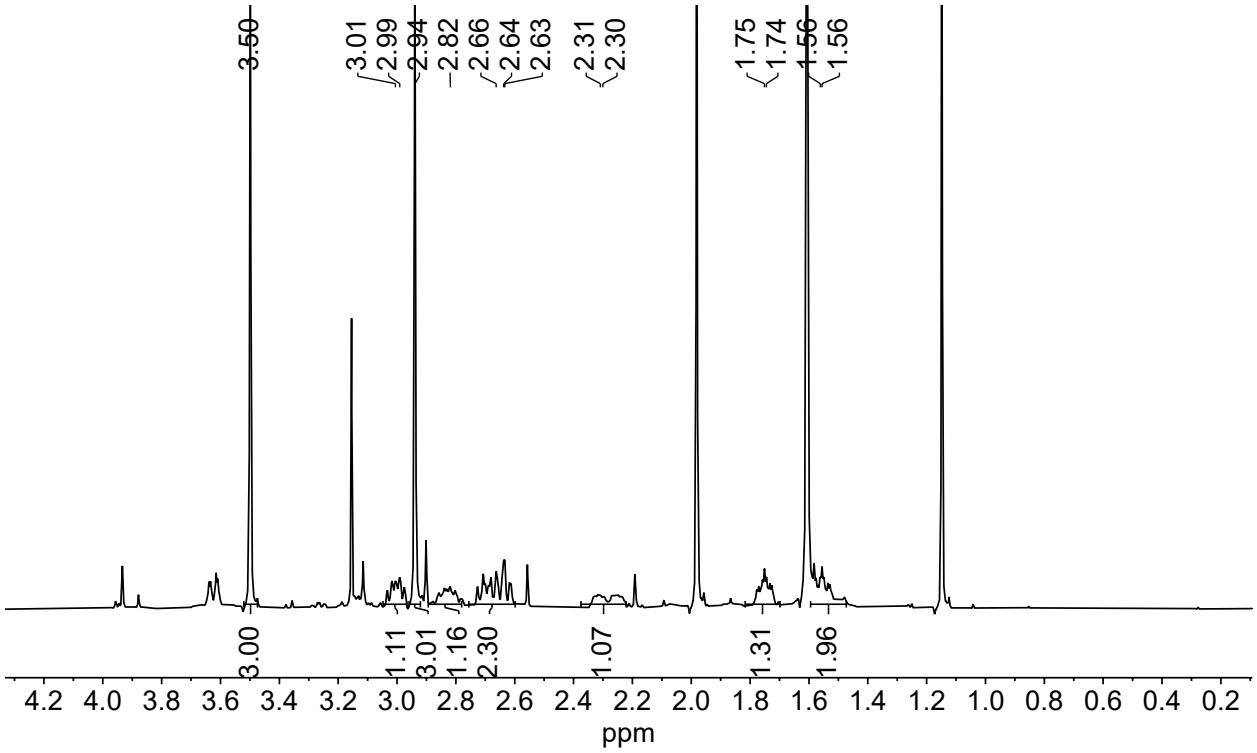

Figure S21. ^{1}H NMR (600 MHz, CD_2Cl_2) spectrum of **4d** with expanded aliphatic region.

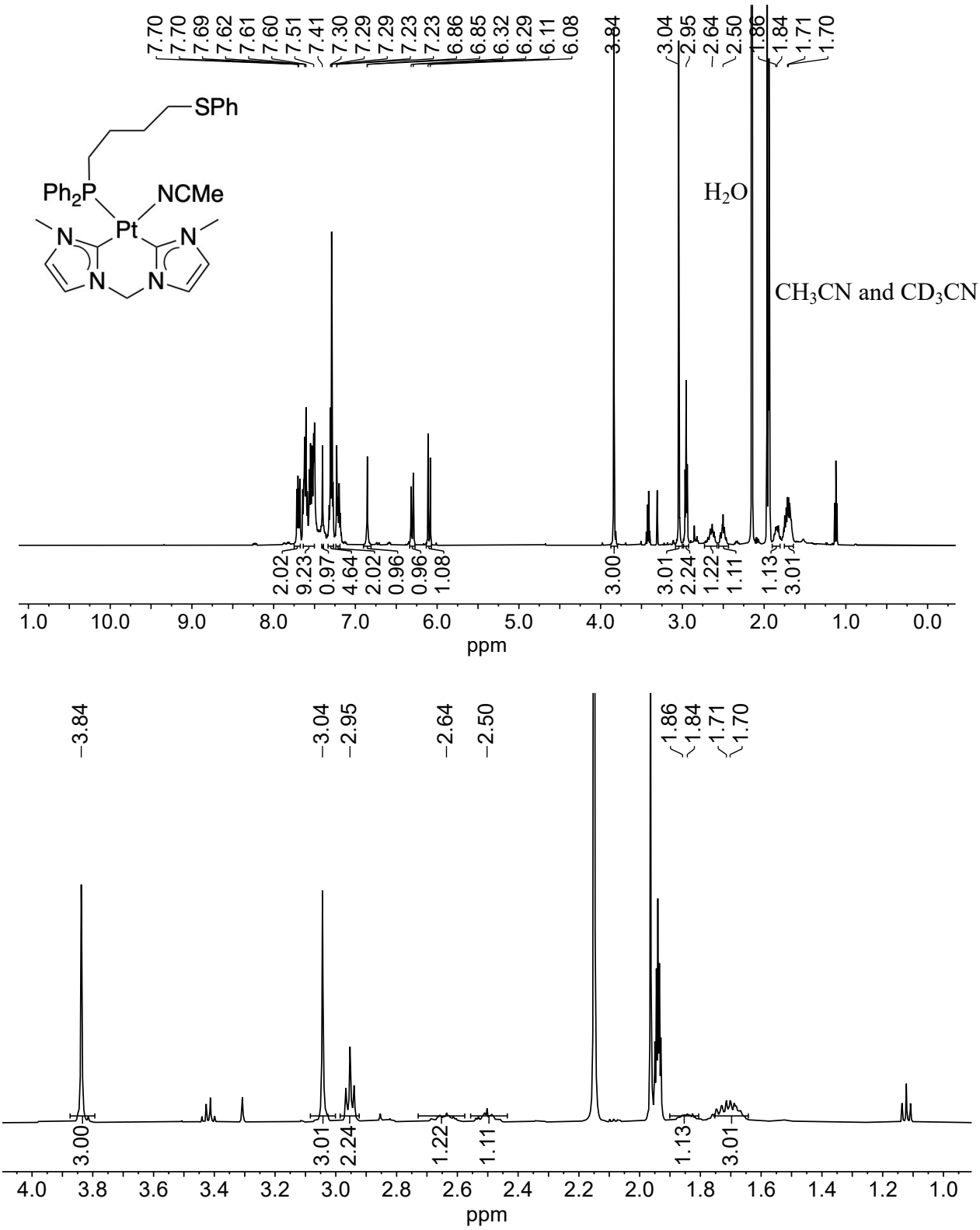

Figure S22. ^{1}H NMR (600 MHz, CD_3CN) spectrum of **5d** with expanded aliphatic region.

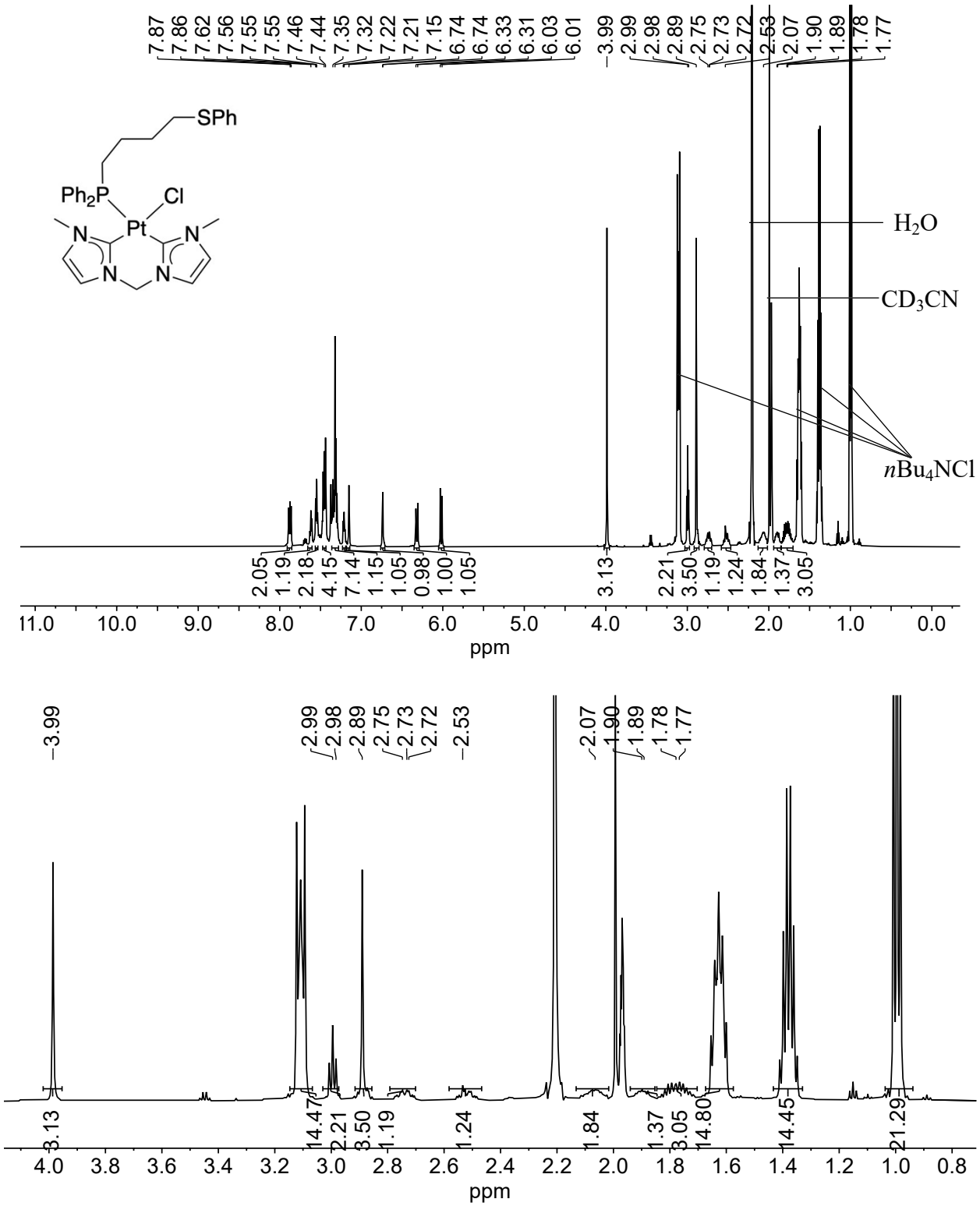

Figure S23. ^{1}H NMR (600 MHz, CD_3CN) spectrum of **6d** with expanded aliphatic region (excess nBu$_4$NCl).

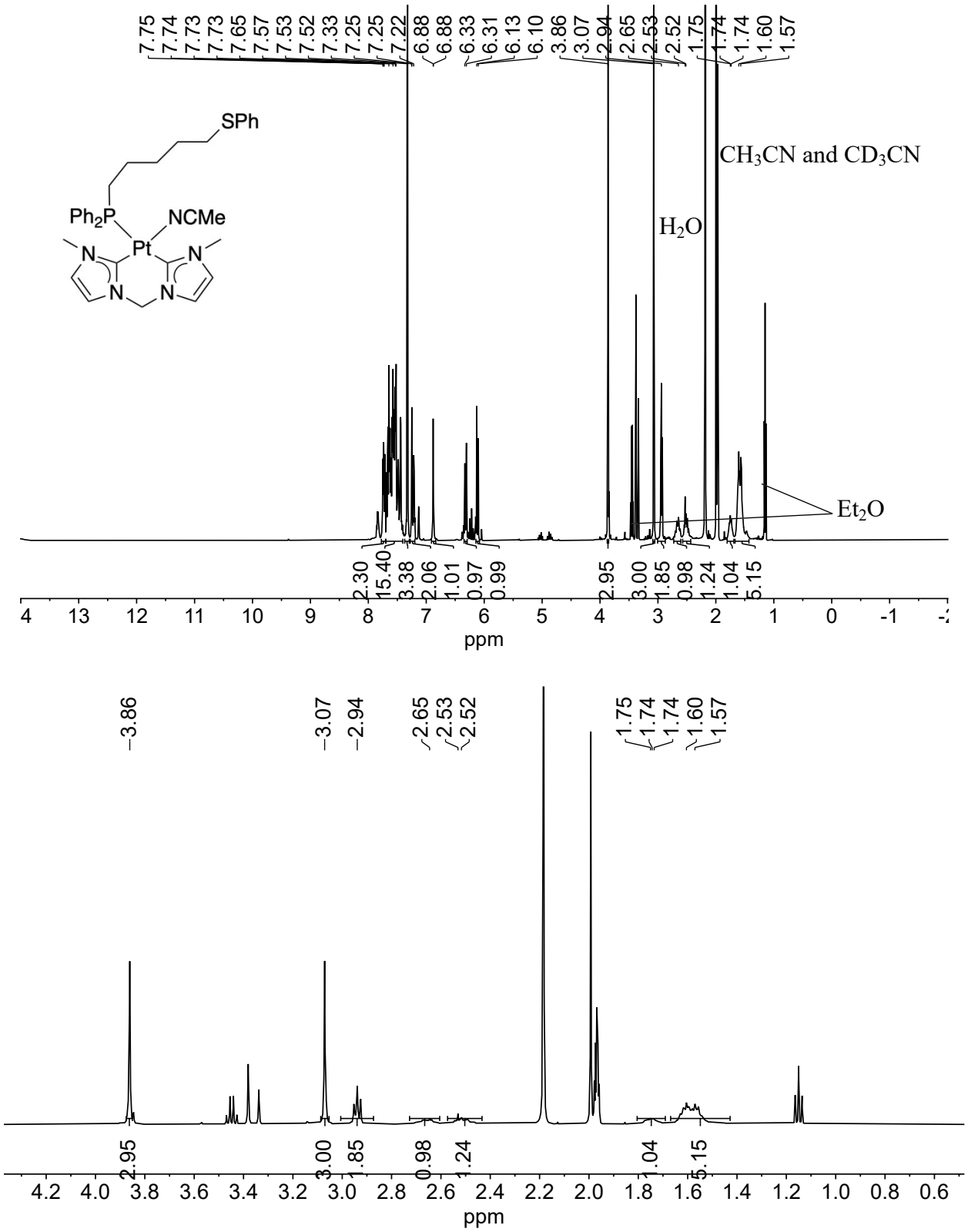

Figure S24. ^{1}H NMR (500 MHz, CD_3CN) spectrum of **5e** with expanded aliphatic region.

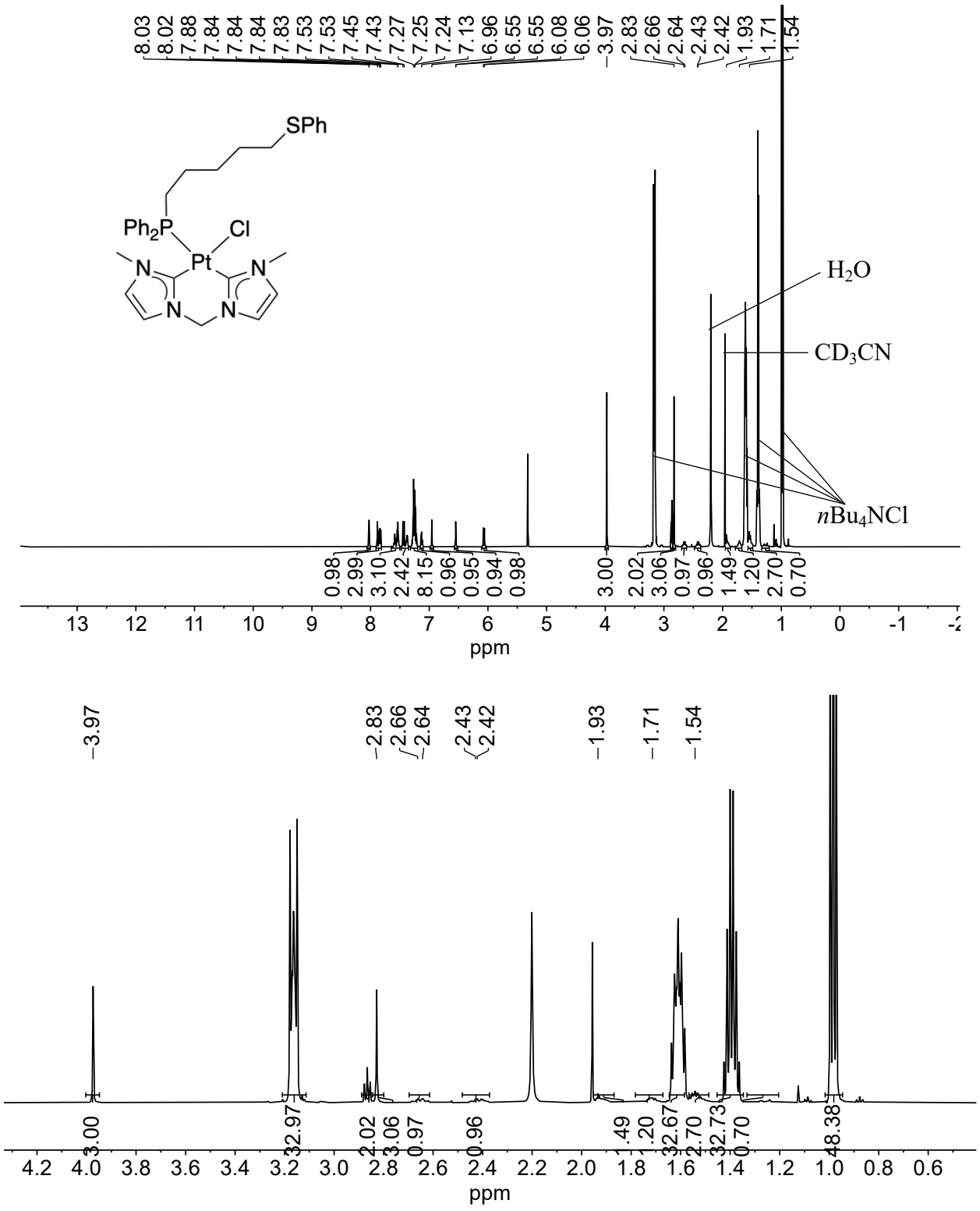

Figure S25. ^{1}H NMR (600 MHz, CD_2Cl_2) spectrum of **6e** with expanded aliphatic region (excess nBu$_4$NCl).

References

(1) Horn, A.; Dussault, P. H. Synthesis of α-Cyano and α-Sulfonyl Cyclic Ethers via Intramolecular Reactions of Peroxides with Sulfone- and Nitrile-Stabilized Carbanions. *J. Org. Chem* **2019**, *84* (22), 14611-14626.
(2) Alcock, N. W.; Brown, J. M.; Evans, P. L. Phosphinosulphoxide rhodium complexes. Synthesis, crystal structure, and catalytic chemistry of [(2,3,5,6-η)-bicyclo[2.2.1]-hepta-2,5-diene][P,O-diphenyl(phenylsulphinylmethyl)-phosphine]rhodium(I) trifluoromethanesulphonate and asymmetric analogues. *J. Organomet. Chem* **1988**, *356* (2), 233-247.
(3) Rigo, P.; Bressan, M. Cyanide complexes of nickel(II) with hybrid bidentate ligands containing phosphorus and nitrogen or sulfur donor atoms. *Inorg. Chem.* **1975**, *14* (7), 1491-1494.
(4) Wiester, M. J.; Braunschweig, A. B.; Yoo, H.; Mirkin, C. A. Solvent and Temperature Induced Switching Between Structural Isomers of RhI Phosphinoalkyl Thioether (PS) Complexes. *Inorg. Chem.* **2010**, *49* (15), 7188-7196.
(5) Block, M.; Kluge, T.; Bette, M.; Schmidt, J.; Steinborn, D. On the Reactivity of Rhodium(I) Complexes with κP-Coordinated γ-Phosphino-Functionalized Propyl Phenyl Sulfide Ligands: Routes to Cyclic Rhodium Complexes with κC,κP- and κP,κS-Coordinated Ligands as Well as Bis(diphenylphosphino)methanide Ligands. *Organometallics* **2010**, *29* (24), 6749-6762.
(6) Ahrens, S.; Strassner, T. Detour-free synthesis of platinum-bis-NHC chloride complexes, their structure and catalytic activity in the CH activation of methane. *Inorganica Chim. Acta* **2006**, *359* (15), 4789-4796.
(7) Bárta, O.; Pinter, P.; Císařová, I.; Strassner, T.; Štěpnička, P. Synthesis and Characterization of Cationic Platinum(II) Complexes with Two Chelating Ligands. *Eur. J. Inorg. Chem.* **2020**, *2020* (6), 575-580.
(8) Delley, B. An all-electron numerical method for solving the local density functional for polyatomic molecules. *J. Chem. Phys.* **1990**, *92* (1), 508-517.
(9) Perdew, J. P.; Burke, K.; Ernzerhof, M. Generalized Gradient Approximation Made Simple. *Phys. Rev. Lett.* **1996**, *77* (18), 3865-3868.
(10) Tkatchenko, A.; Scheffler, M. Accurate Molecular Van Der Waals Interactions from Ground-State Electron Density and Free-Atom Reference Data. *Phys. Rev. Lett.* **2009**, *102* (7), 073005.
(11) Fulmer, G. R.; Miller, A. J. M.; Sherden, N. H.; Gottlieb, H. E.; Nudelman, A.; Stoltz, B. M.; Bercaw, J. E.; Goldberg, K. I. NMR Chemical Shifts of Trace Impurities: Common Laboratory Solvents, Organics, and Gases in Deuterated Solvents Relevant to the Organometallic Chemist. *Organometallics* **2010**, *29* (9), 2176-2179.